Monsoons, plumes, and blooms:
intraseasonal variability in the subsurface chlorophyll fluorescence of the Bay of Bengal

Tamara Schlosser, Andrew J Lucas, Melissa Omand, J Thomas Farrar

Coupled air-sea interactions

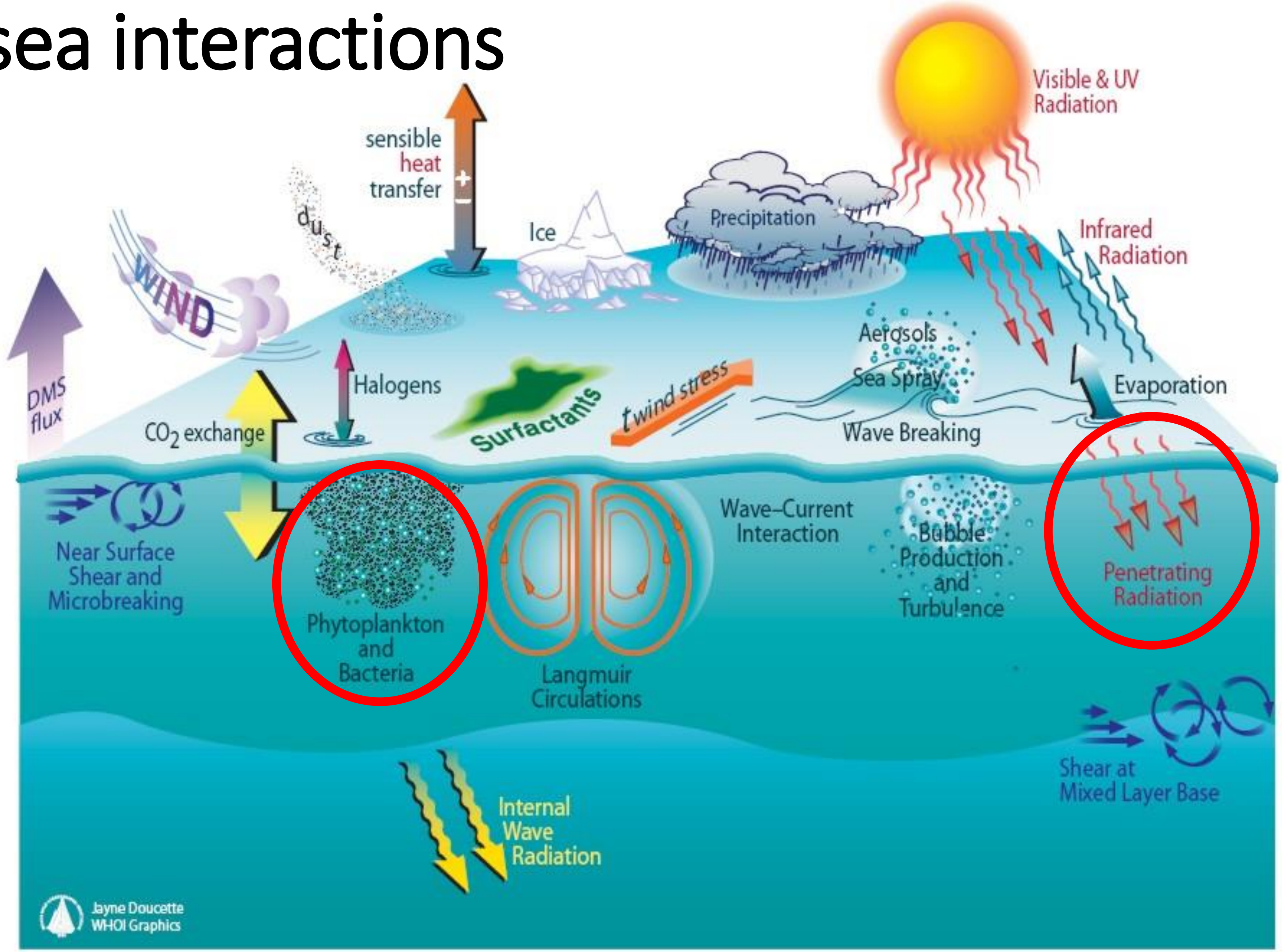

Accounting for ‘biothermal feedback’

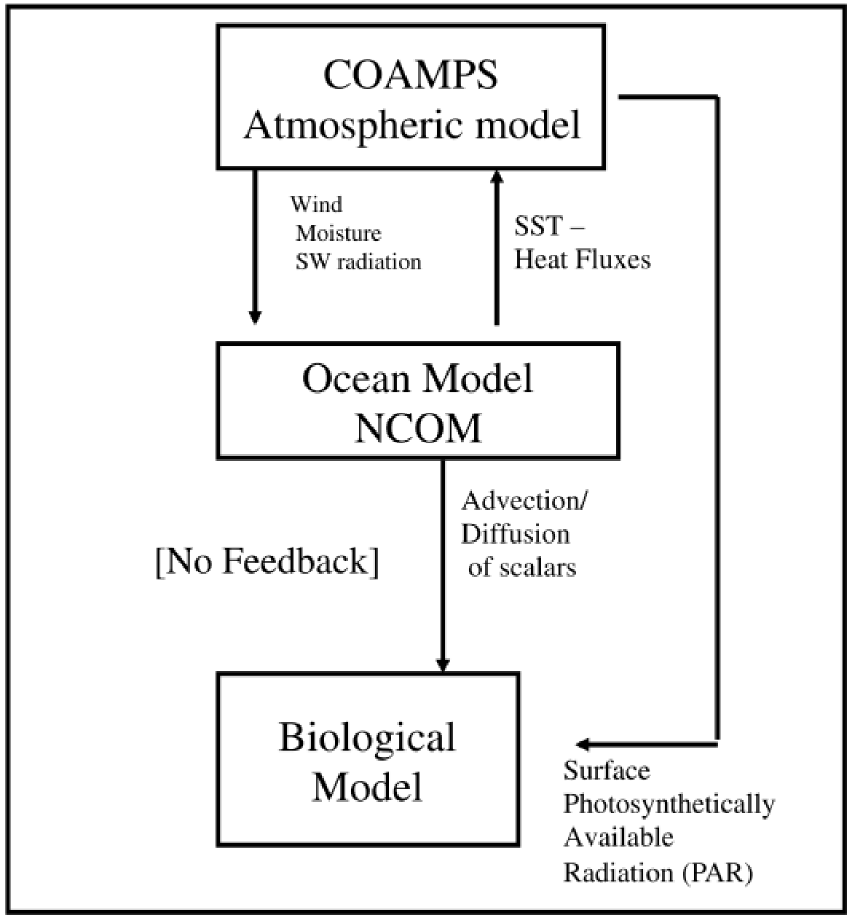

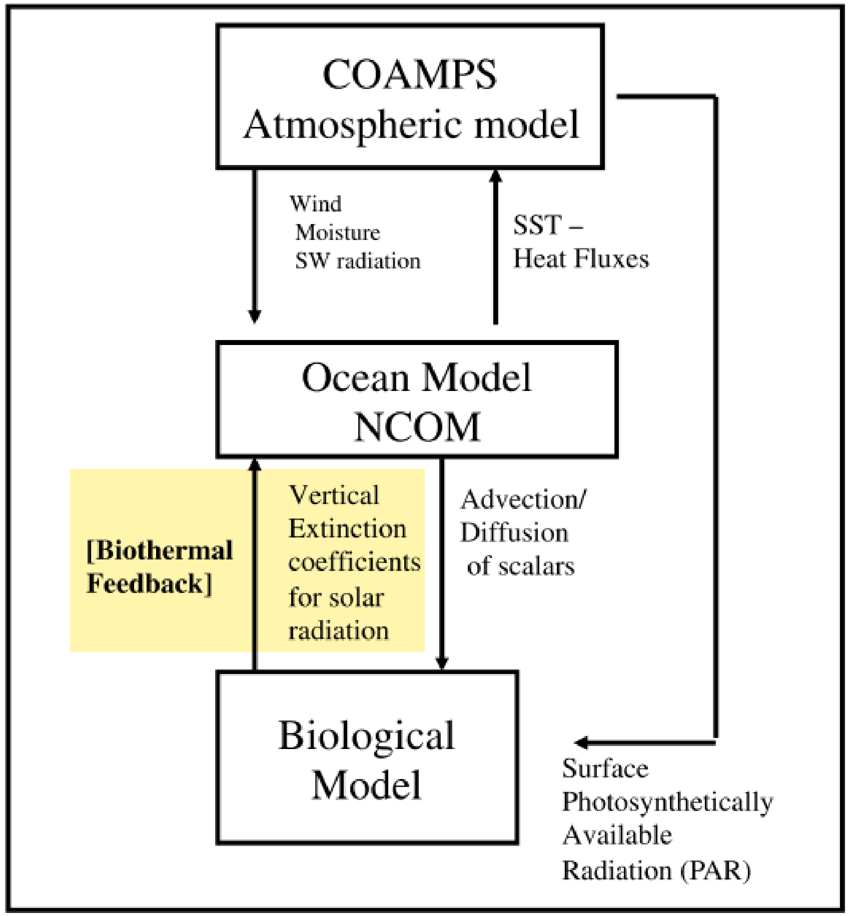

(Joliff & Smith 2013)

The details of penetrative radiation can significantly change SST and air temp: Biothermal feedback in Monterey Bay

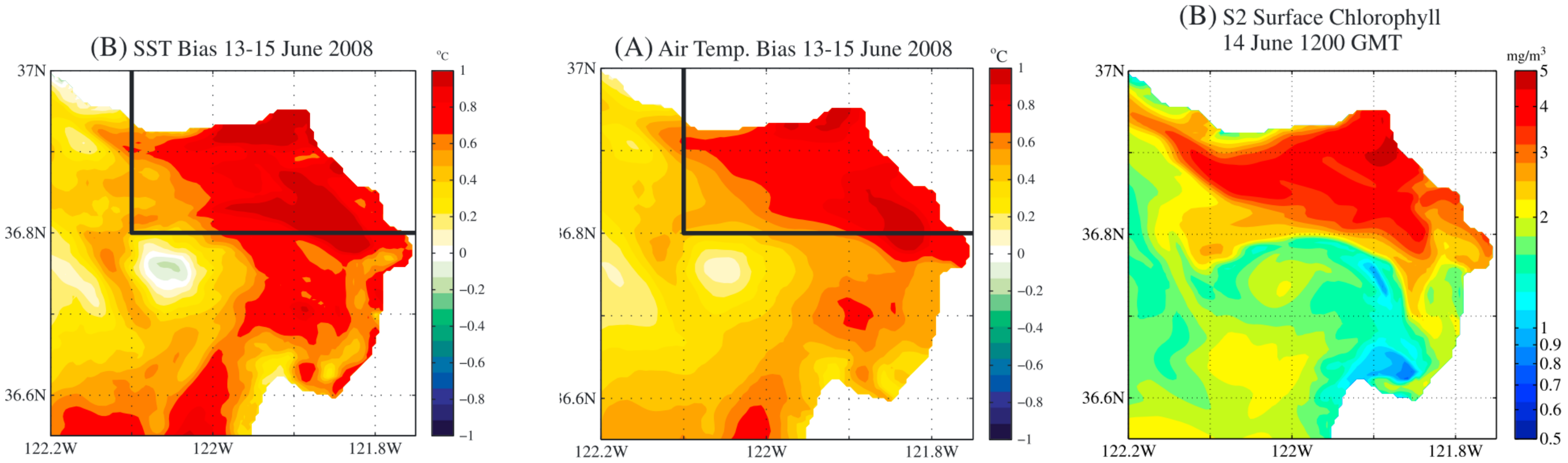

(Joliff & Smith 2013)

- Accounting for the chlorophyll (Chl) impact on penetrative radiation resulted in bias in SST, air temperature, relative humidity, wind speeds, and surface Chl
- That's in Monterey - what does the analogous situation look like in the BoB?

Chl and the marine food chain

- Phytoplankton growth is limited by photon fluxes (i.e., light) from above and nutrient fluxes from below
- Phytoplankton require visible light, or photosynthetically available radiation (PAR), to photosynthesize
- In the open ocean, nitrogen (N) typically limits phytoplankton growth
- Phytoplankton represent the base of the marine food-chain

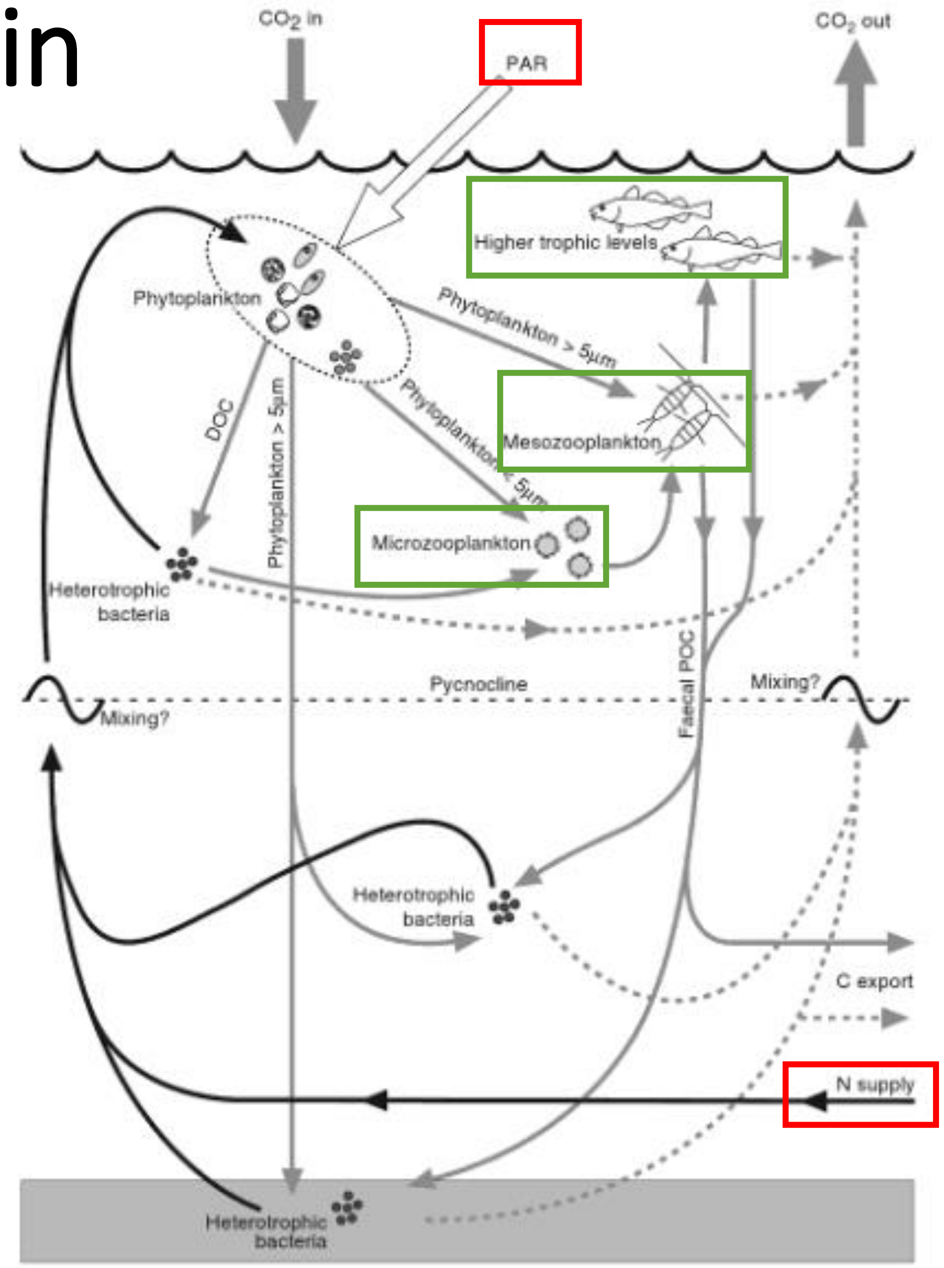

(Simpson & Sharples 2012)

Chl and the carbon cycle

- The autotrophic fixation of carbon is driven by PAR and determines the biologically mediated fluxes of carbon between the atmosphere, the long-term storage pools of carbon in slope sediments, and the deep ocean (Simpson & Sharples 2012)

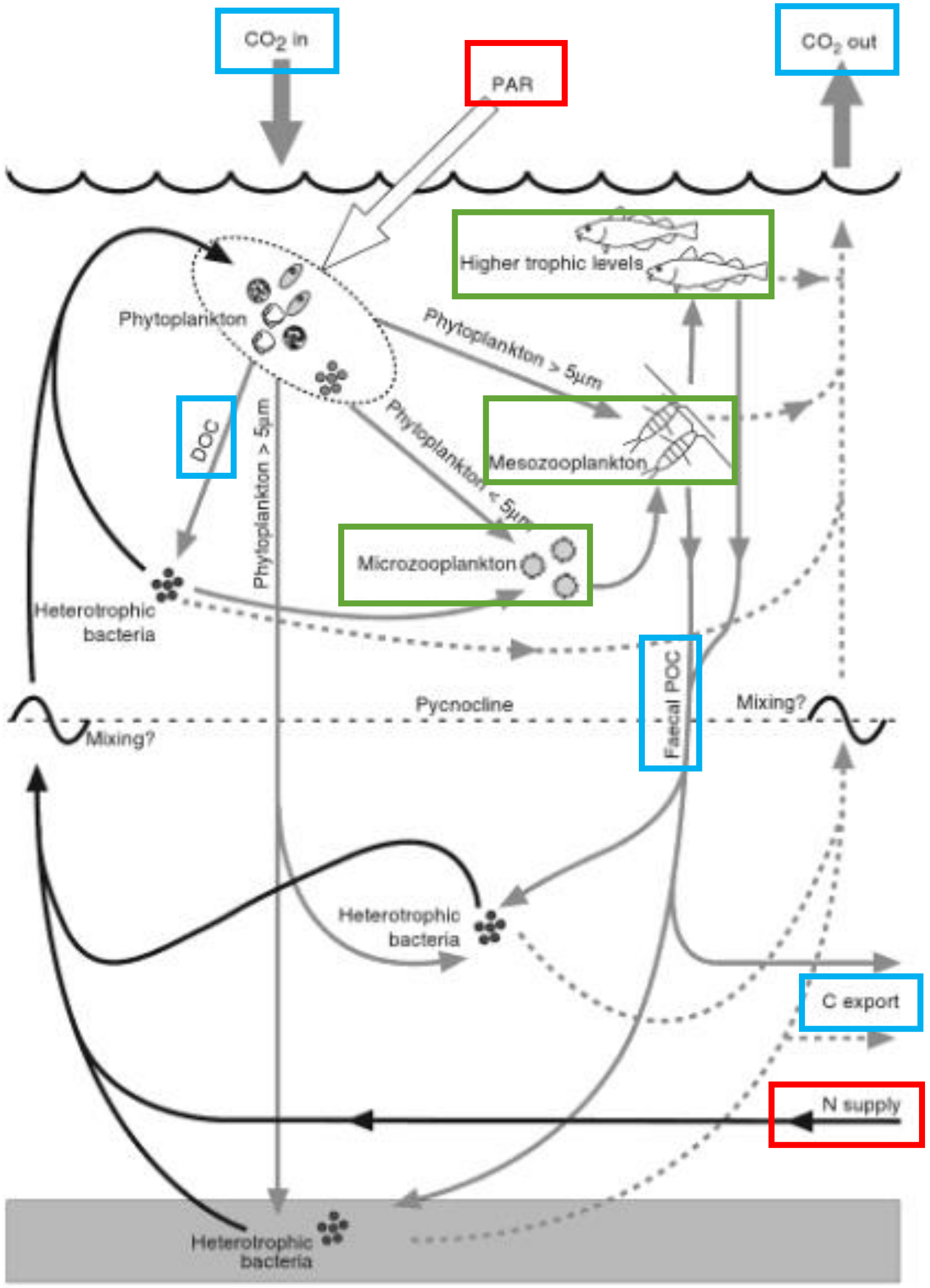

(Simpson & Sharples 2012)

Chl, irradiance, and the heat budget

This subroutine computes the balance of heat in the form

$$\dot{\Theta} = \boxed{\mathcal{D}_\Theta} - \frac{1}{\tau_R^\Theta}(\Theta - \Theta_{obs}) + \boxed{\frac{1}{C_p\rho_0}\frac{\partial I}{\partial z}}\ , \tag{27}$$

where $\dot{\Theta}$ denotes the material derivative of the mean potential temperature Θ, and $\mathcal{D}_\Theta$ is the sum of the turbulent and viscous transport terms modelled according to

$$\mathcal{D}_\Theta = \frac{\partial}{\partial z}\left(\boxed{(\nu_t^\Theta + \nu^\Theta)}\frac{\partial\Theta}{\partial z} - \tilde{\Gamma}_\Theta\right) \quad . \tag{28}$$

In this equation, ν_t^Θ and ν^Θ are the turbulent and molecular diffusivities of heat, respectively, and $\tilde{\Gamma}_\Theta$ denotes the non-local flux of heat, see section 4.

(Umlauf et al. 2006)

- Where $I(z)$ is the subsurface irradiance
- The heat flux profile is usually determined more by wind mixing than by radiation absorption alone (Price et al. 1986)

Bio-physical interactions

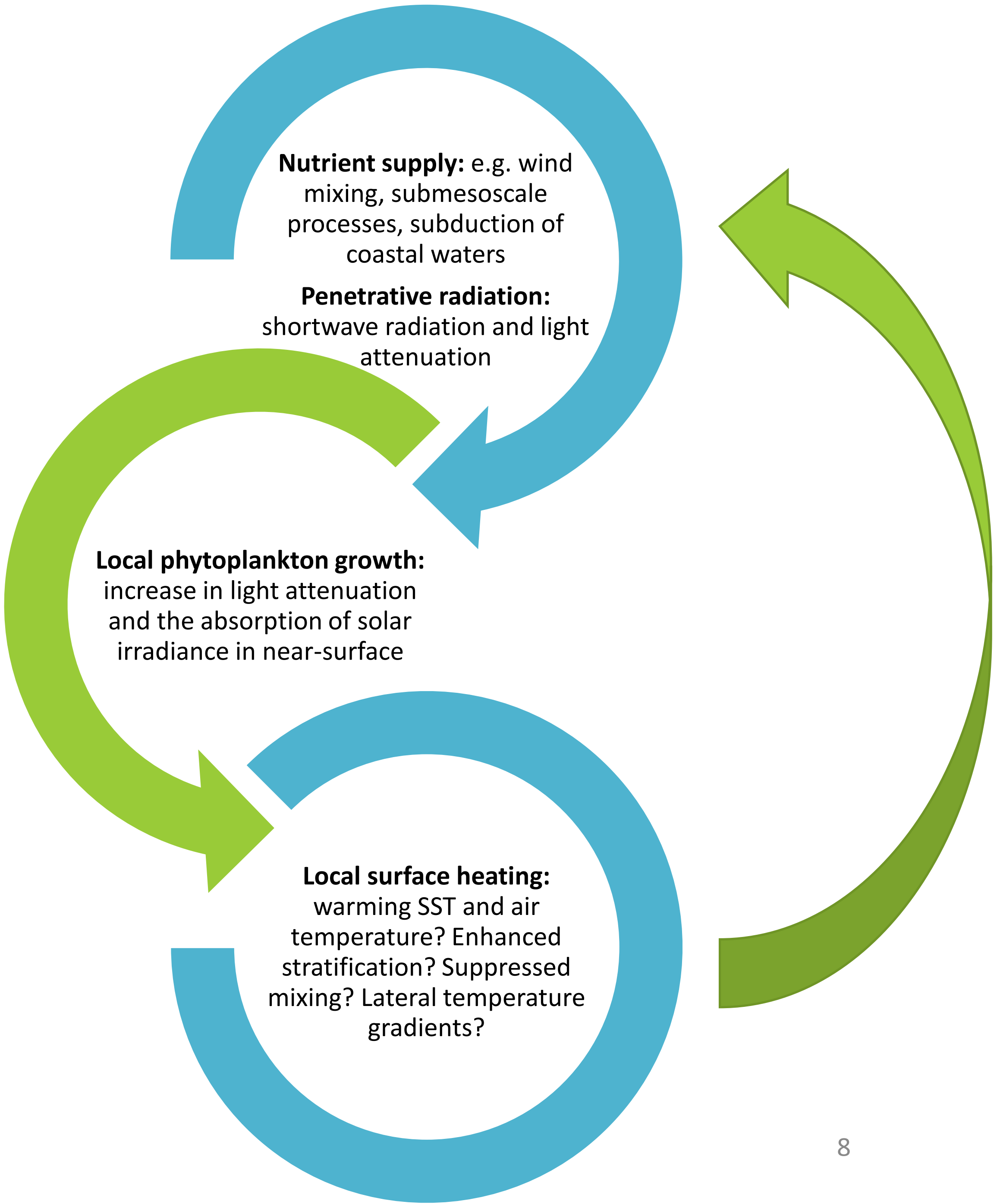

Light-limited phytoplankton growth within the Bay of Bengal during the southwest monsoon (Schlosser et al. in preparation)

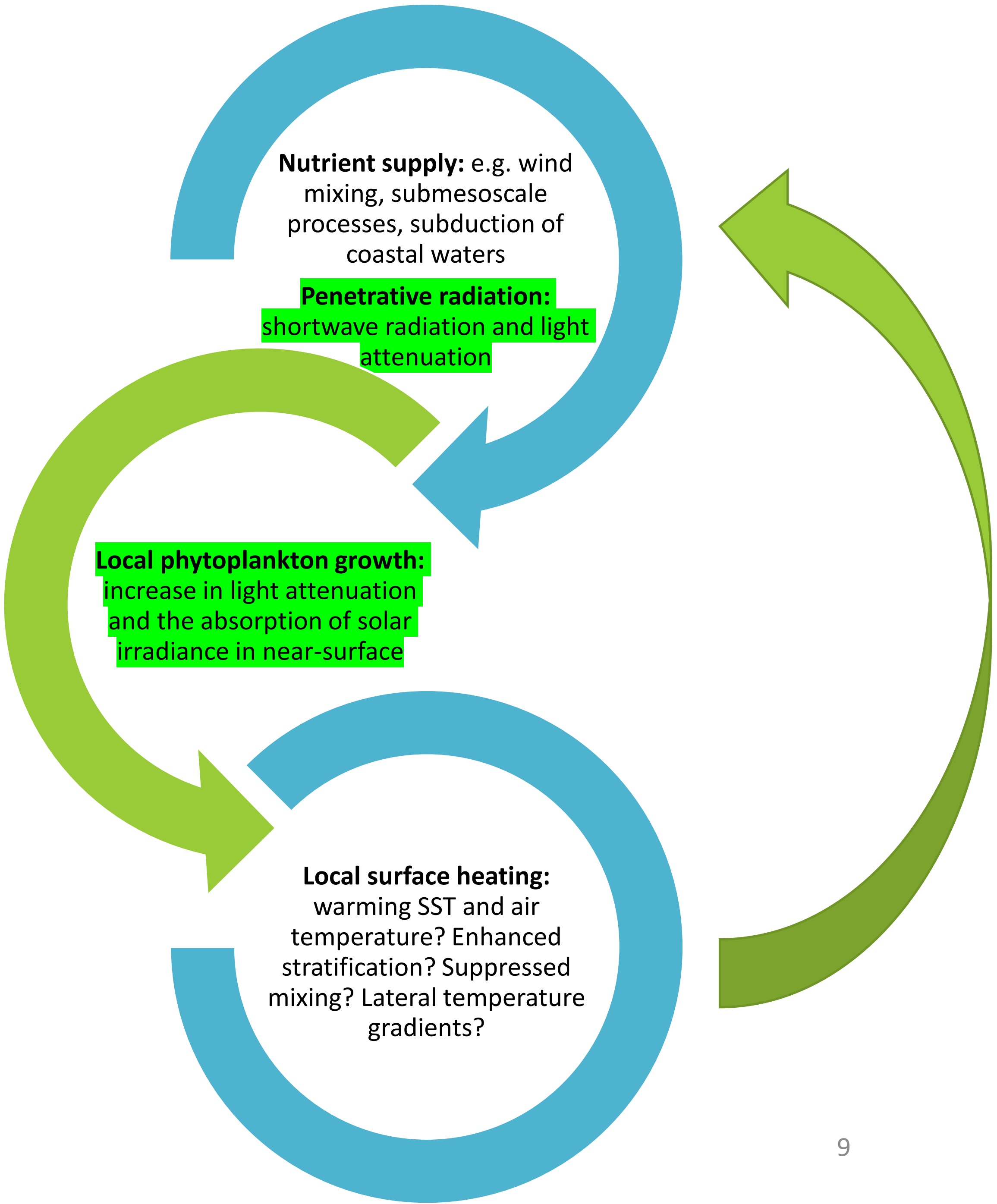

Light-limited phytoplankton growth within the Bay of Bengal during the southwest monsoon (Schlosser et al. in preparation)

Impact of time-variable light attenuation on the upper-ocean heat budget in the Bay of Bengal within one-dimensional coupled air-sea models.
(Future work)

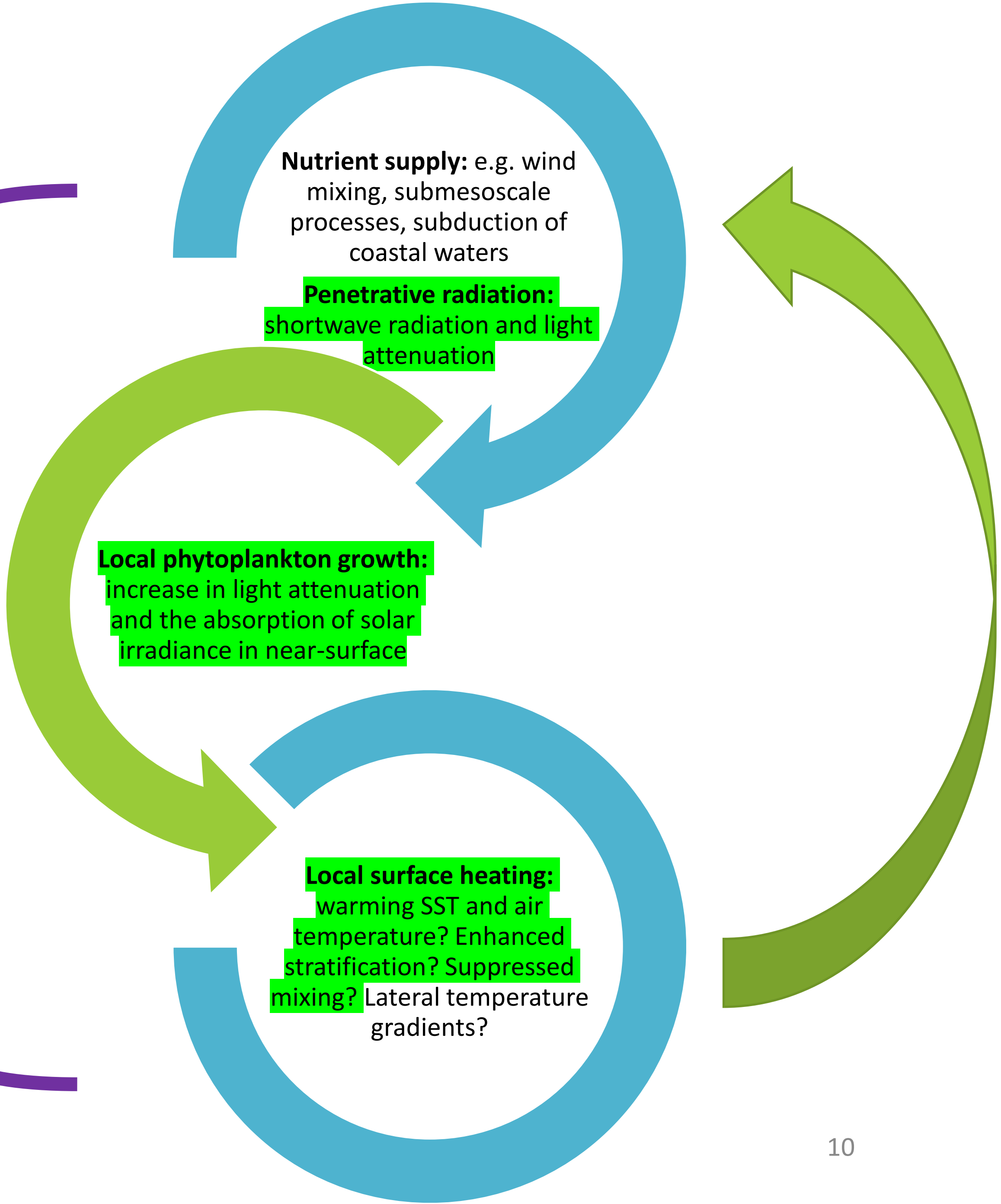

Background: Subsurface irradiance

$$I(z) = I(0)[R\exp(-K_1 z) + (1 - R)\exp(-K_2 z)]$$

$I(0)$: surface irradiance

R: proportion non-visible vs. visible radiation

K_1: non-visible light attenuation
(also diffuse attenuation)

K_2: visible light attenuation

(e.g. Price et al. 1986)

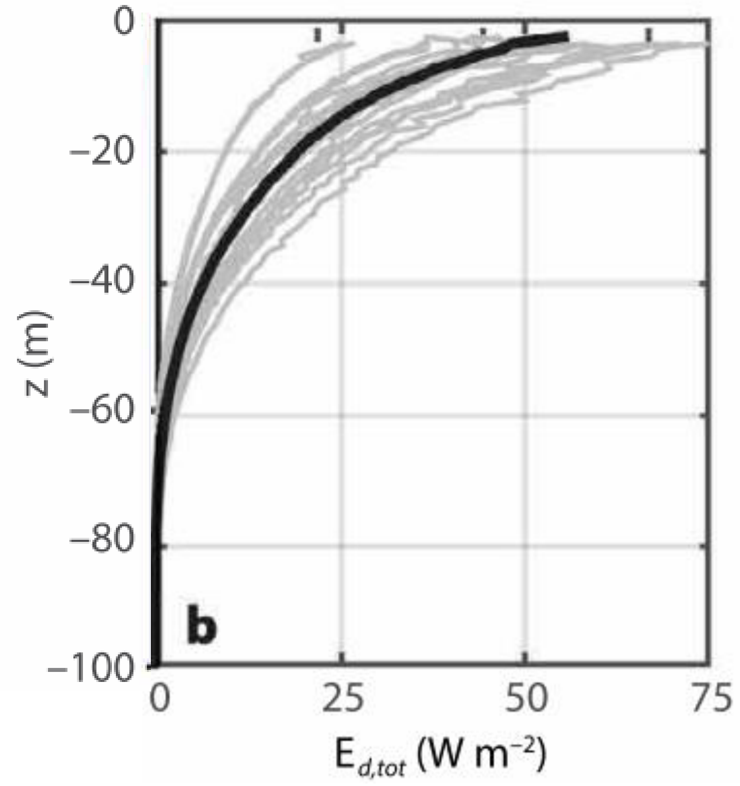

(Lotliker et al. 2016)

Light attenuation

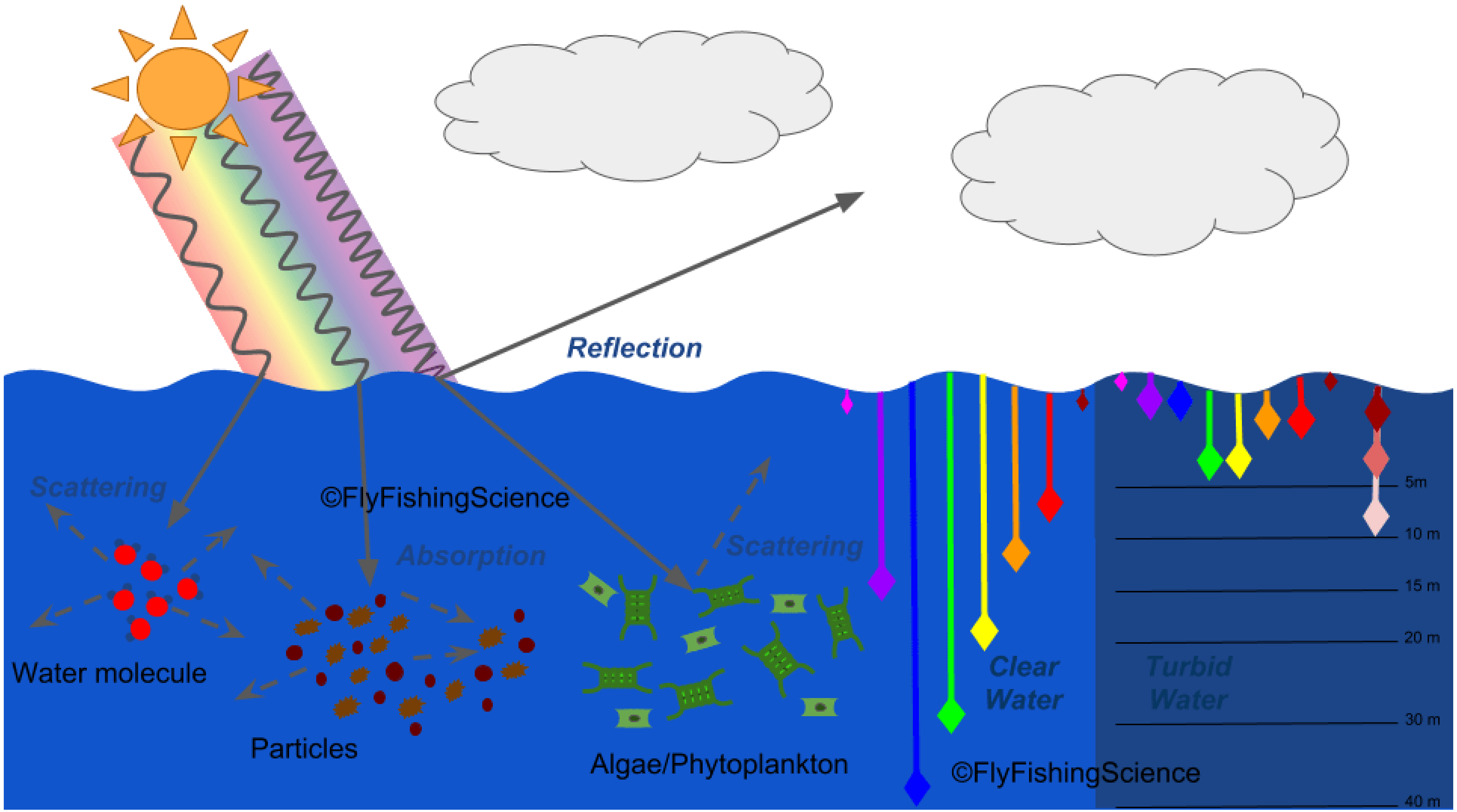

https://flyfishingscience.co.uk/2018/10/19/light-attenuation-in-water/

Jerlov water types

$$I(z) = I(0)[R\exp(-K_1 z) + (1 - R)\exp(-K_2 z)]$$

$I(0)$: surface irradiance

R: proportion non-visible vs. visible radiation

K_1: non-visible light attenuation

K_2: visible light attenuation

(e.g. Price et al. 1986)

Jerlov (1968) water types	R	K_1 (m)	K_2 (m)
Type 1 – relatively clear	0.58	0.35	23
Type 1 (upper 50 m)	0.68	1.2	28
Type 1A	0.62	0.60	20
Type 1B	0.67	1.0	17
Type 2	0.77	1.5	14
Type 3 – murky	0.78	1.4	7.9

Time- and depth-variability

$$\cancel{I(z) = I(0)[R\exp(-K_1 z) + (1 - R)\exp(-K_2 z)]}$$

$$I(z,t) = I(0,t)[R(t)\exp(-K_1(z,t)z) + (1 - R(t))\exp(-K_2(z,t)z)]$$

Clouds

Water clarity

$I(0)$: surface irradiance

R: proportion non-visible vs. visible radiation

K_1: non-visible light attenuation

K_2: visible light attenuation

Chl impacts light attenuation

- Observations from southern BoB
- Here K_2 is h_2 and scales with surface chlorophyll-*a* (Chl) concentrations
- K_2 varies by >20 m across the Bay
- $K_2 \propto$ Chl is predicted for Class-1 waters

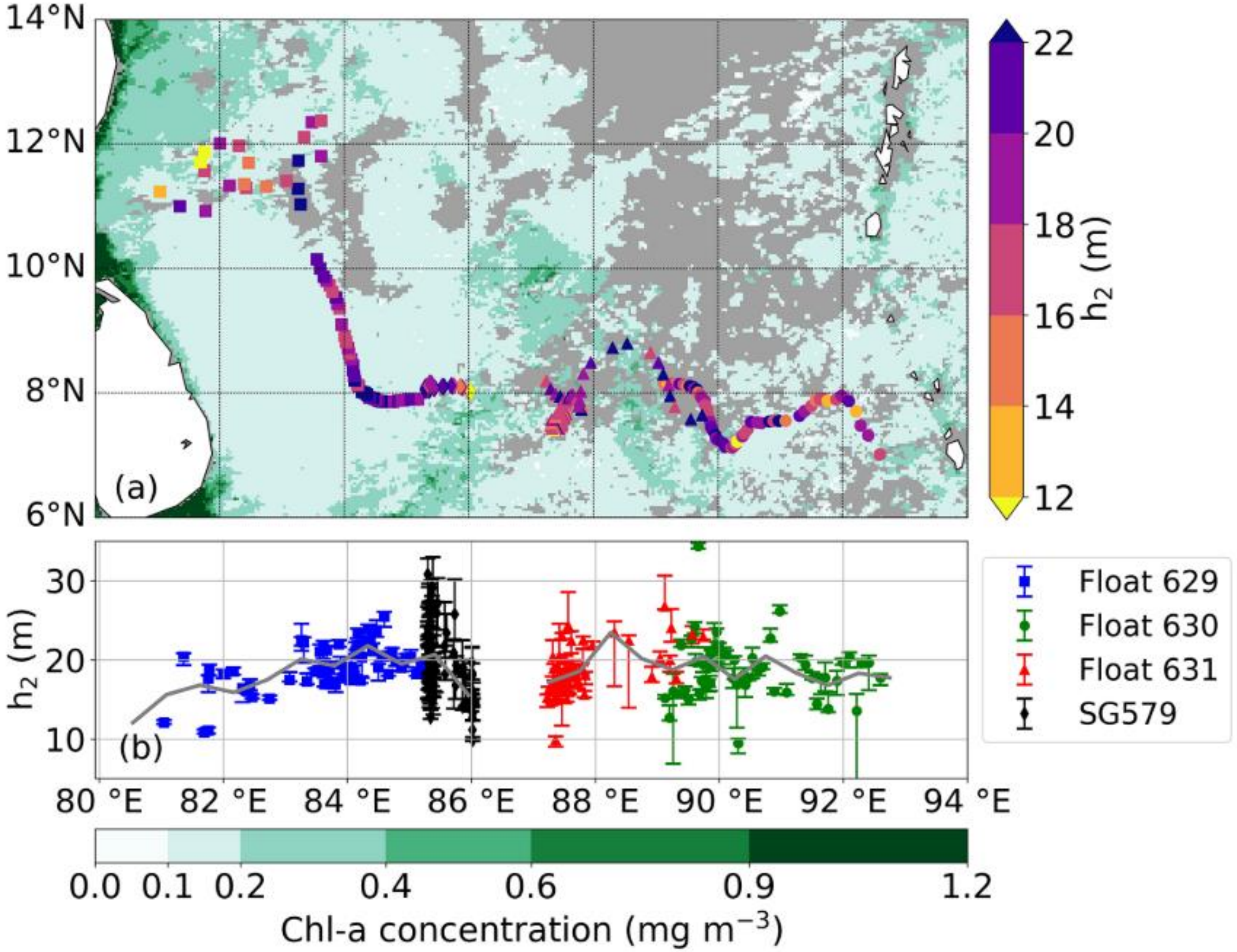

(Giddings et al. 2021)

Light attenuation vs. wavelength

- Here K is inverted and shown for clear waters
- In addition to accounting for the time-, spatial- and depth-variability in light attenuation, we can improve estimates by adding wavelength (λ) resolution to K
- Jerlov water types are convenient and are an approximation that may under-state the influence of time-variable water clarity

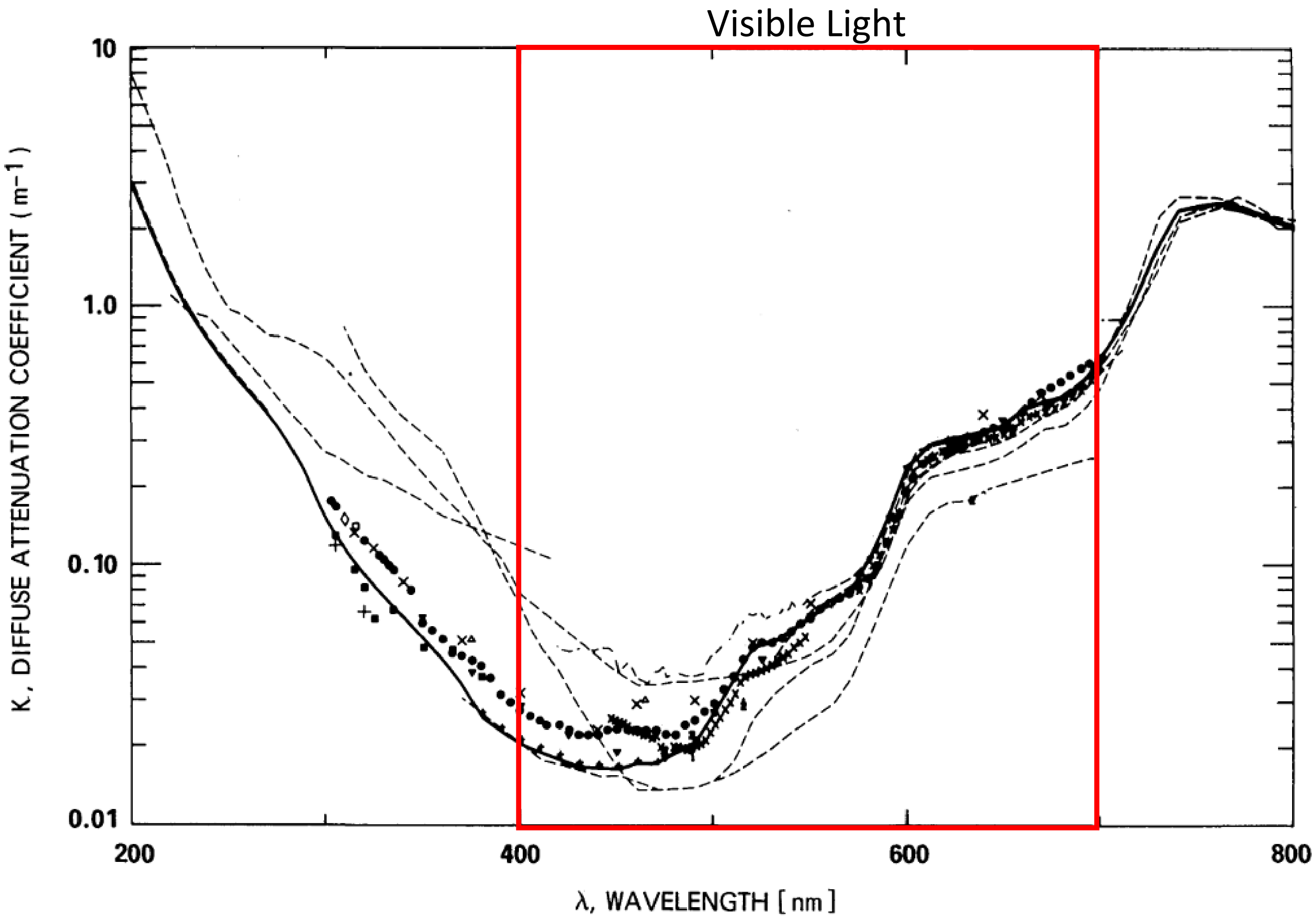

(Smith & Baker 1981)

Measuring subsurface irradiance

- Measuring irradiance over the upper ~5 m is largely impacted by surface waves via wave scattering of light

- Observing R and K_1 is challenging in wavy conditions

- We can observe K_2 at high fidelity from autonomous vehicles like vertical profilers (e.g. Wirewalker) and gliders

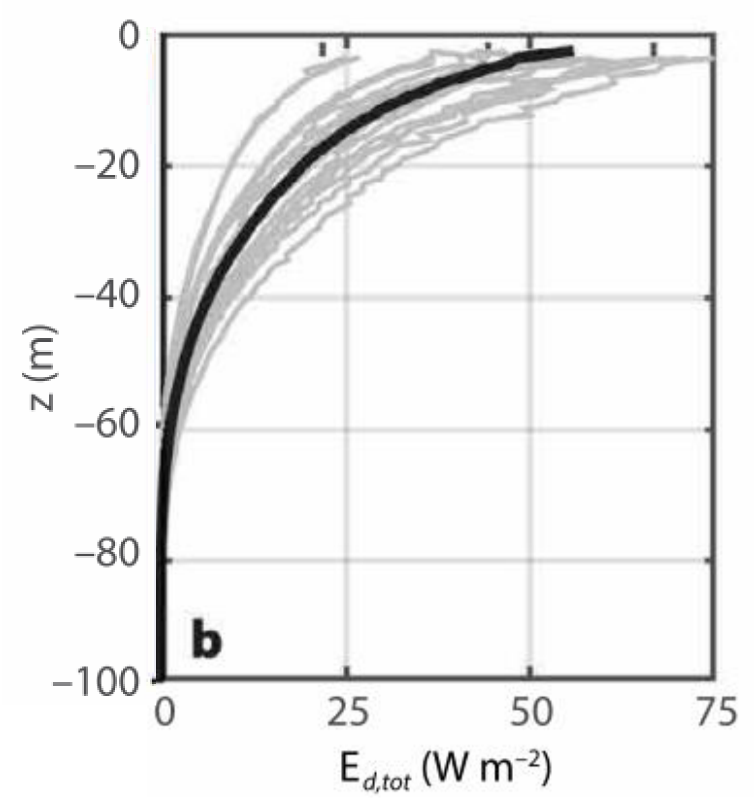

(Lotliker et al. 2016)

Study Site- July 2019 campaign

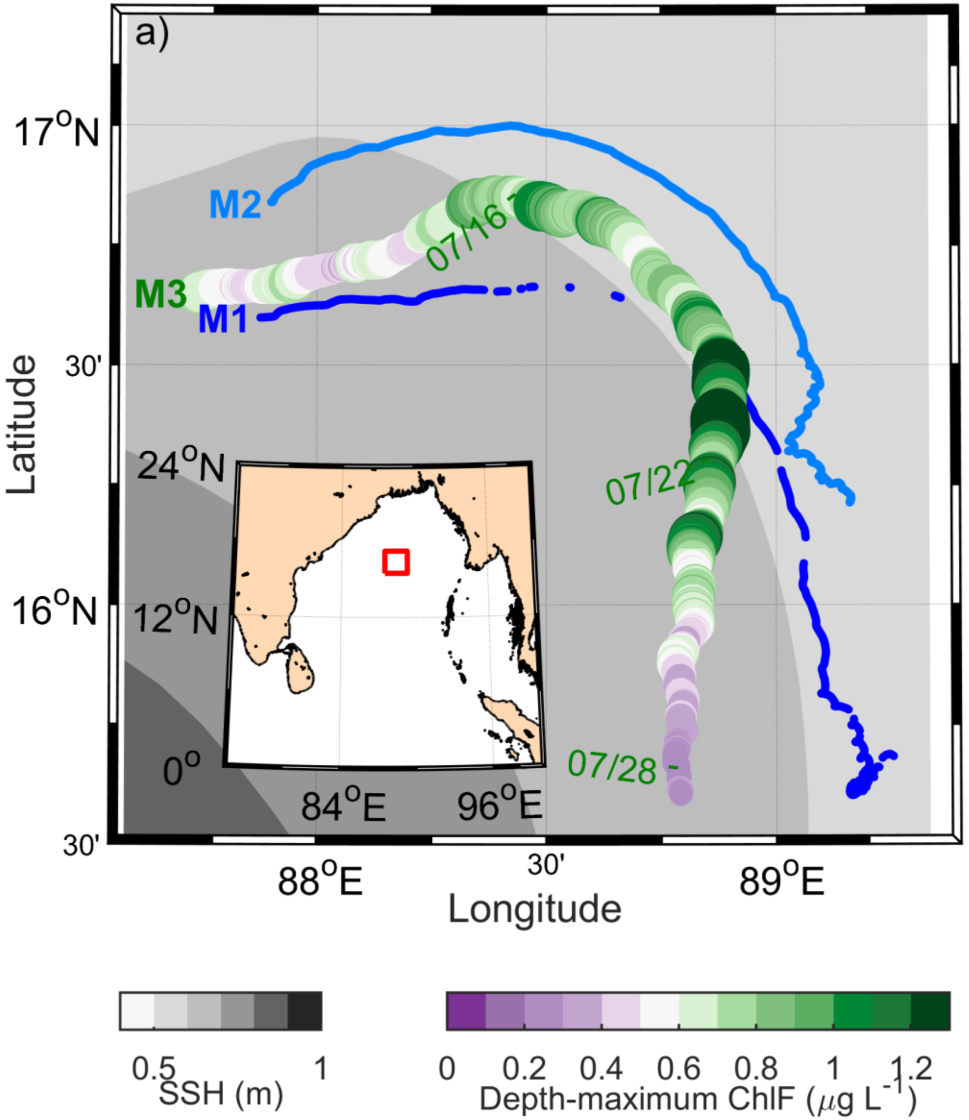

- We deployed 3 vertical profilers for ~18 days in July, 2019

Drogued-Buoy Air Sea Interaction System (D-BASIS)

Instrumentation presented here (subsample of all data):

- WHOI metocean buoy including shortwave radiation (SWR)
- Wirewalker profiling upper 100 m including:
  - CTD
  - Chlorophyll-*a* fluorescence (ChlF), a proxy for the concentration. We did not calibrate in the field so concentrations presented here are not precise.
  - Downward irradiance at wavelengths 380, 412, 490, and 532 nm
  - To estimate photosynthetically available radiation (PAR):

$$PAR(z,t) = \int_{380}^{532} I(z,t)d\lambda \times \frac{700-400}{532-380}$$

  - Optical backscatter- turbidity (NTU)
  - Most variables were telemetered to the ship in real time

MISO BOB V1

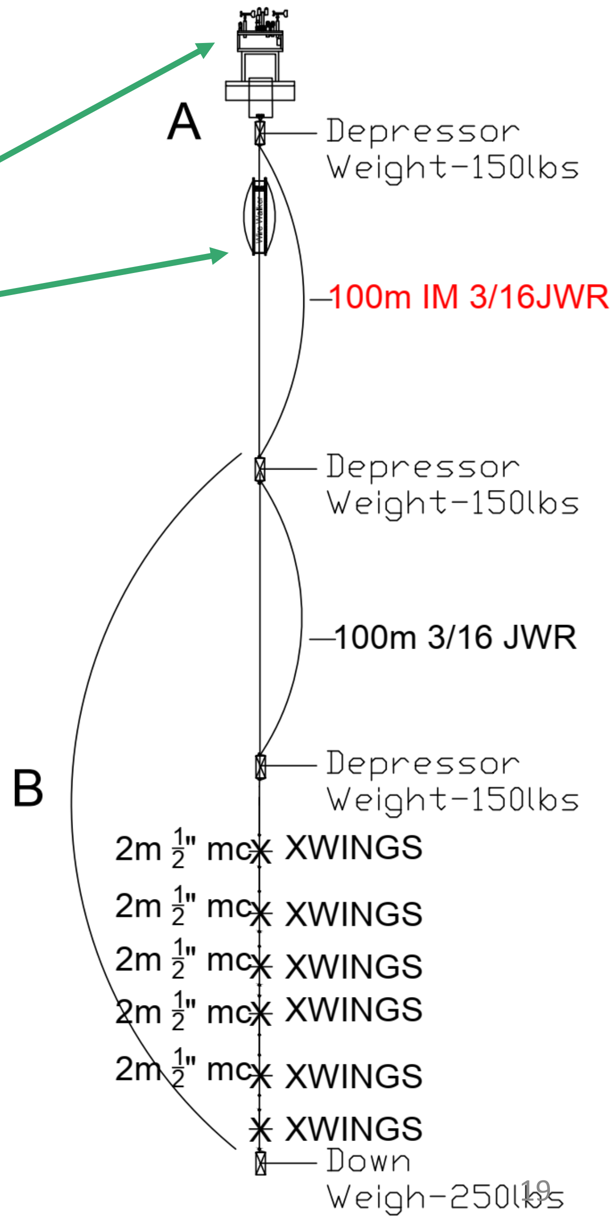

Study Site- July 2019 campaign

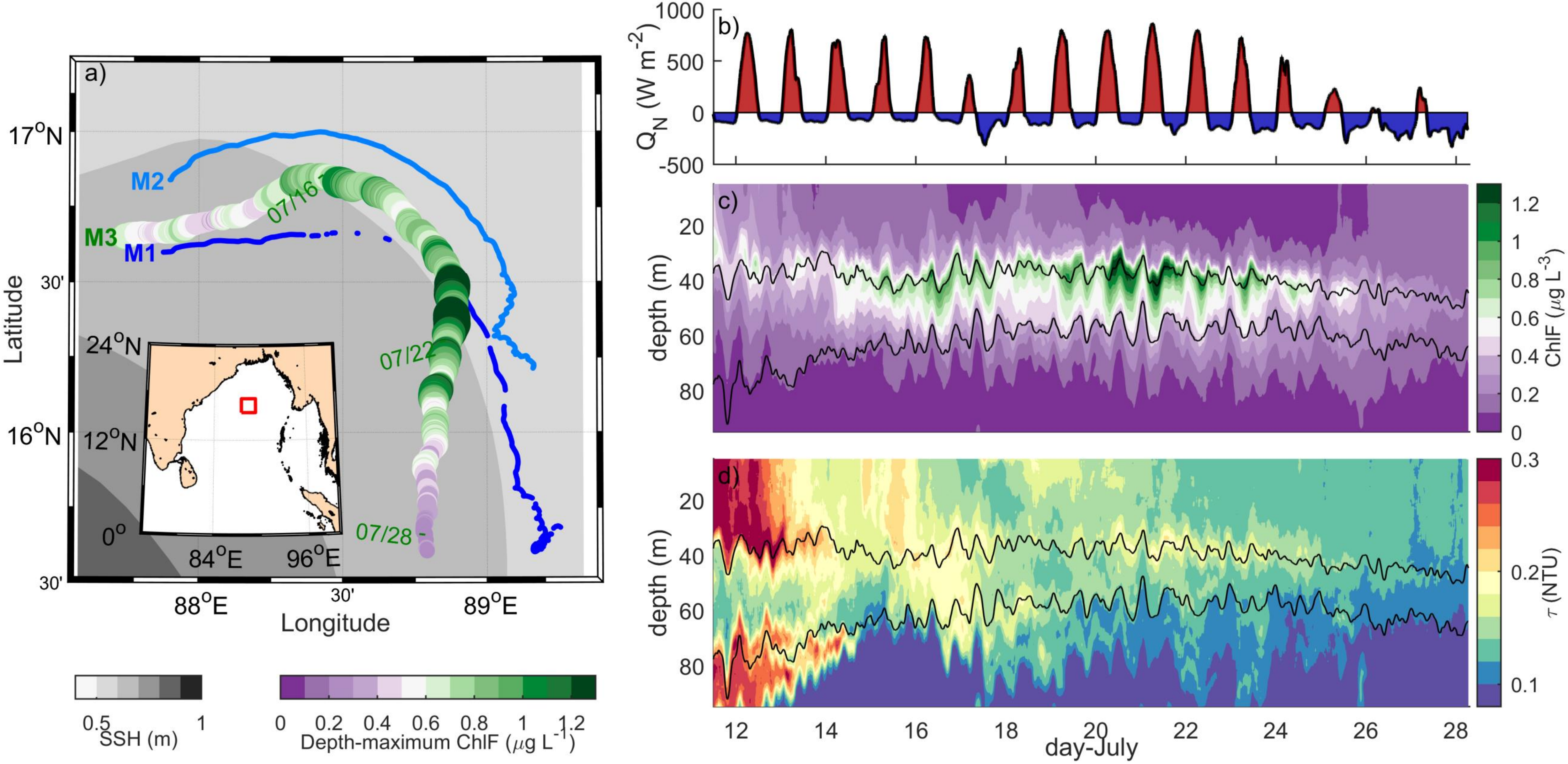

Light Attenuation (*K*)

- Light attenuation varied over depth but here we use a simplified depth-averaged value

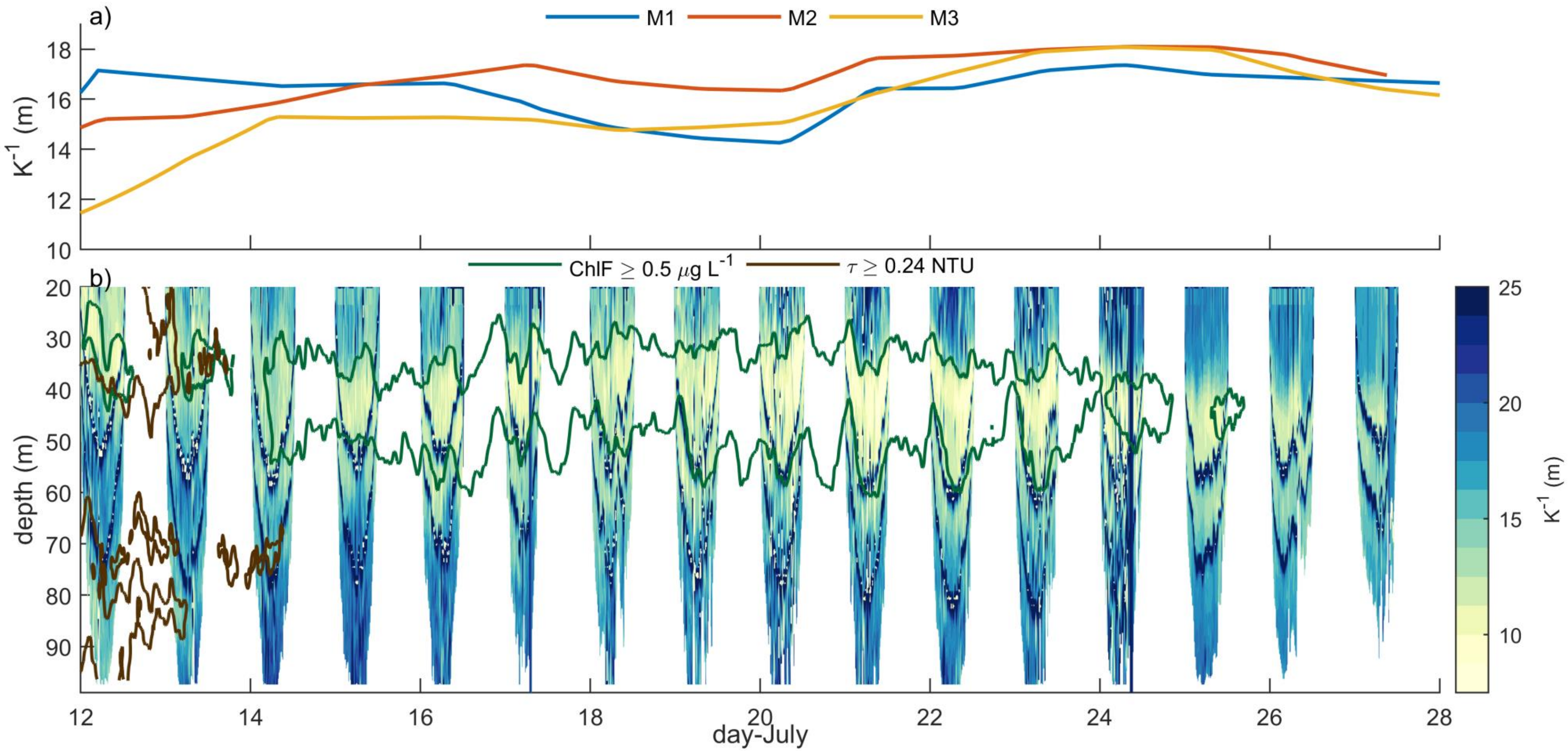

PAR and Chlorophyll fluorescence (ChlF)

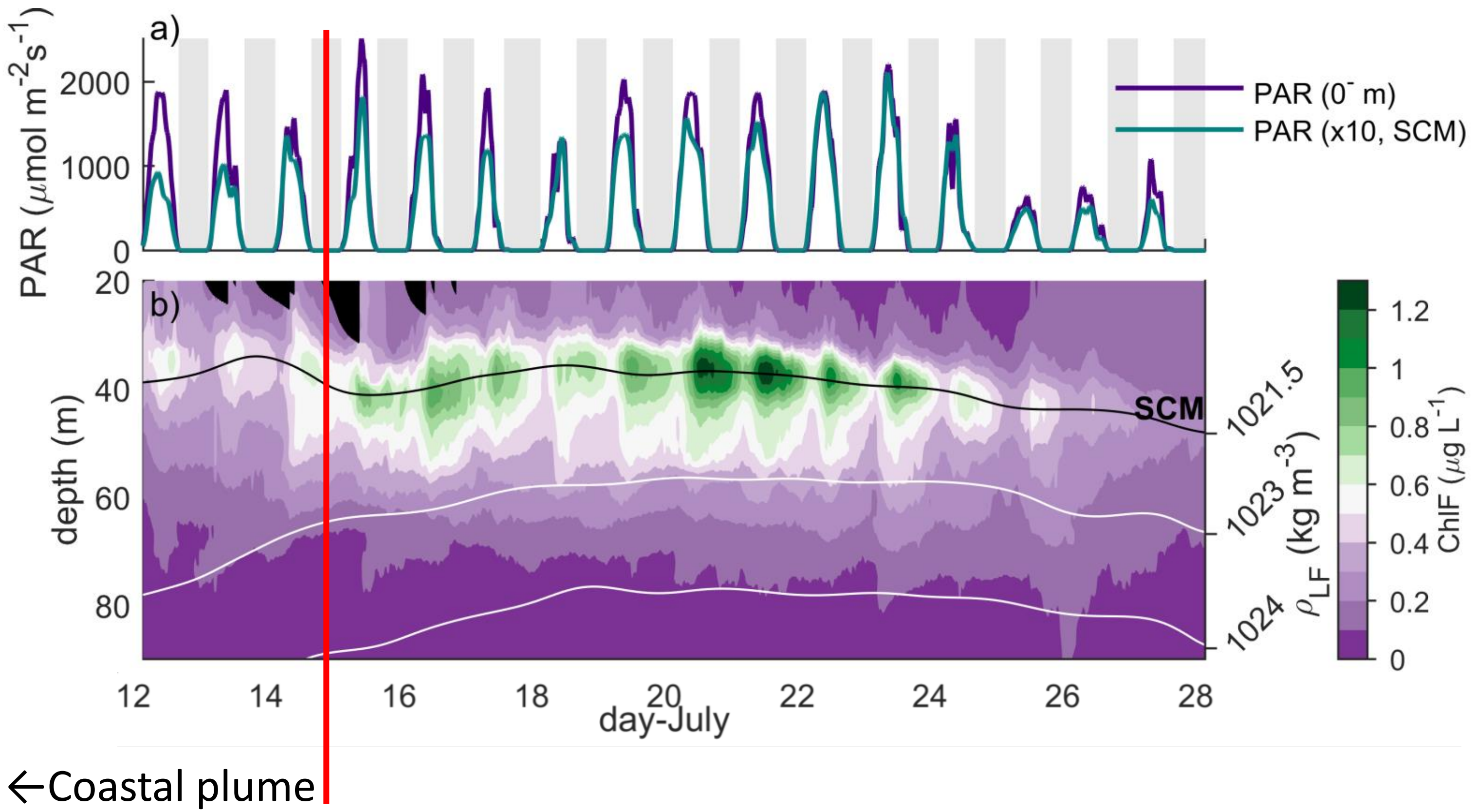

Diel Cycle

- Previously observed in the Bay (Lucas et al. 2016)
- Chl increases with sunlight – we can make use of the coupling between PAR and Chl to estimate the gross production of Chl and the rate of Chl loss

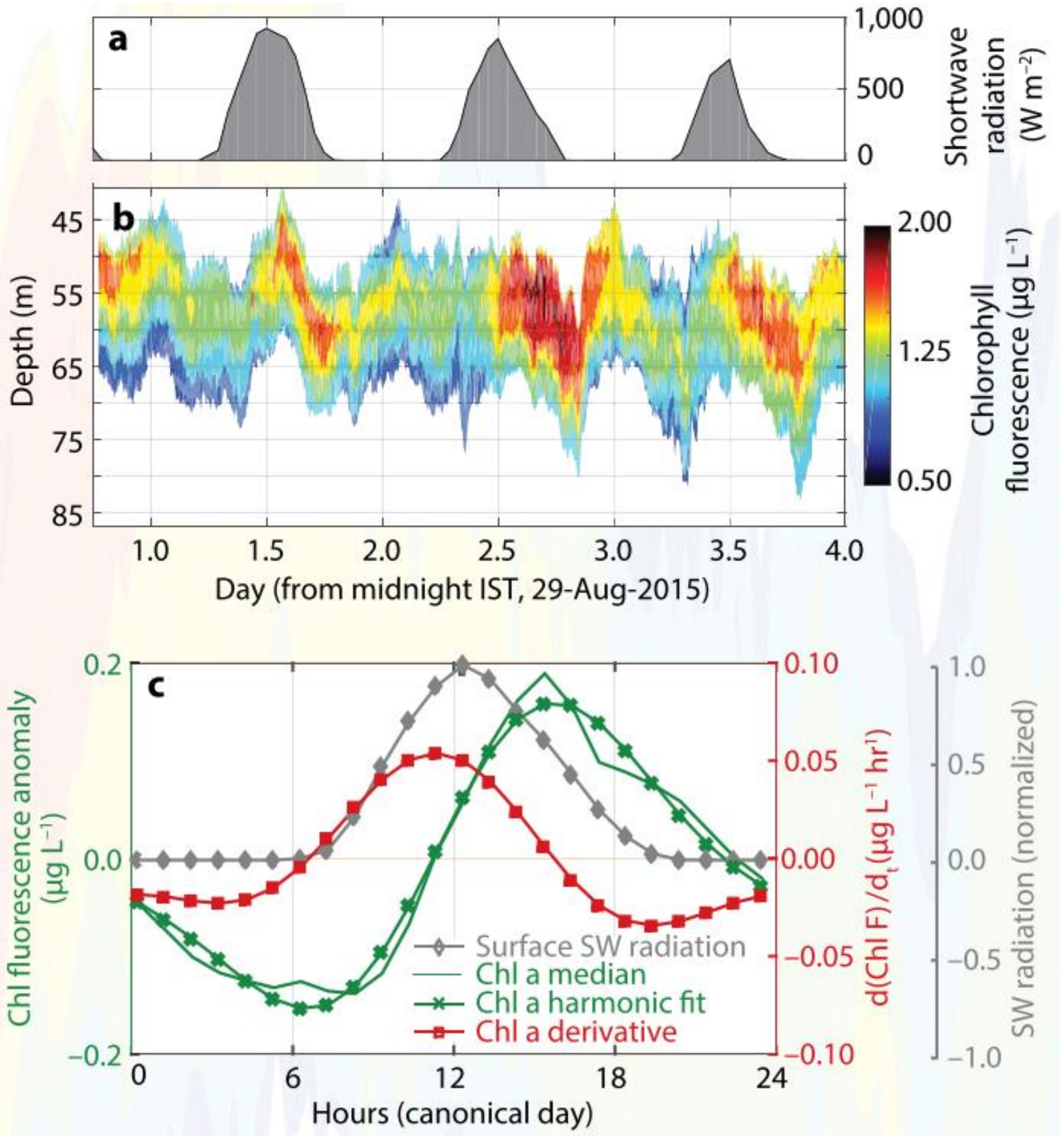

dielFit - https://github.com/duebi/dielFit

dielFit

MATLAB routine to estimate rates of gross production and community respiration from diel measurements of concentration of oxygen, particles, or other parameters. This routine is reported in a manuscript by Barone et al. (2019) and builds on the approach used by Nicholson et al. (2015). Estimates of community rates rely on the assumption of constant respiration throughout the day while the assumption on gross production varies based on three models:

1. Linear model, assuming constant production during daytime
2. Sinusoidal model, assuming that production scales linearly with light intensity
3. P vs. E model, including a parameterization for light saturation and photoinhibition

Rates estimates are obtained using linear least squares while rate uncertainties are obtained by bootstrapping the model residuals. Residual autocorrelation is tested using the Durbin-Watson test.

Observed ChlF

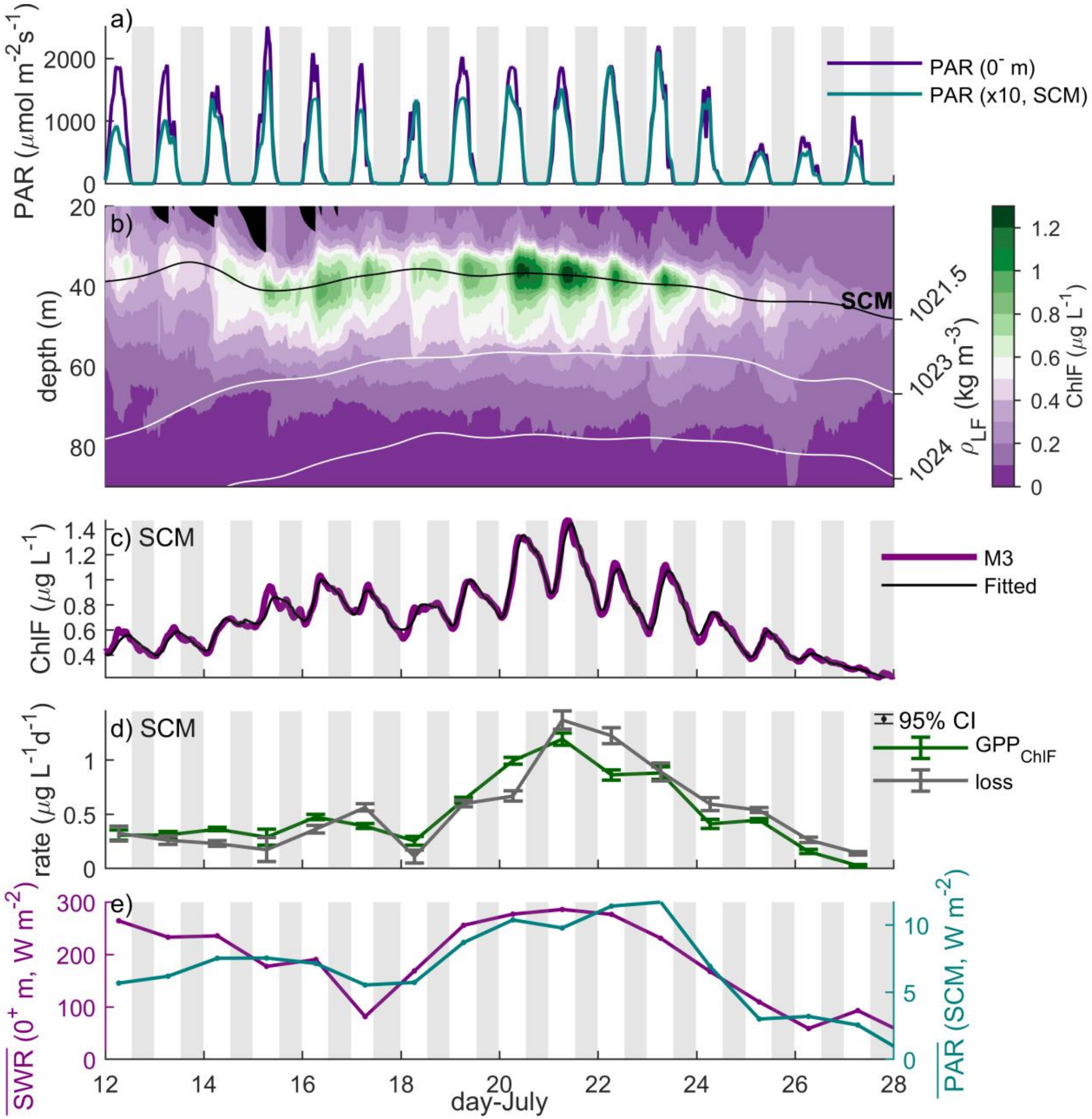

Observed ChlF

- ChlF decreased due to loss>GPP, so still observed large diel cycle in Chl even when the daily averaged Chl decreased

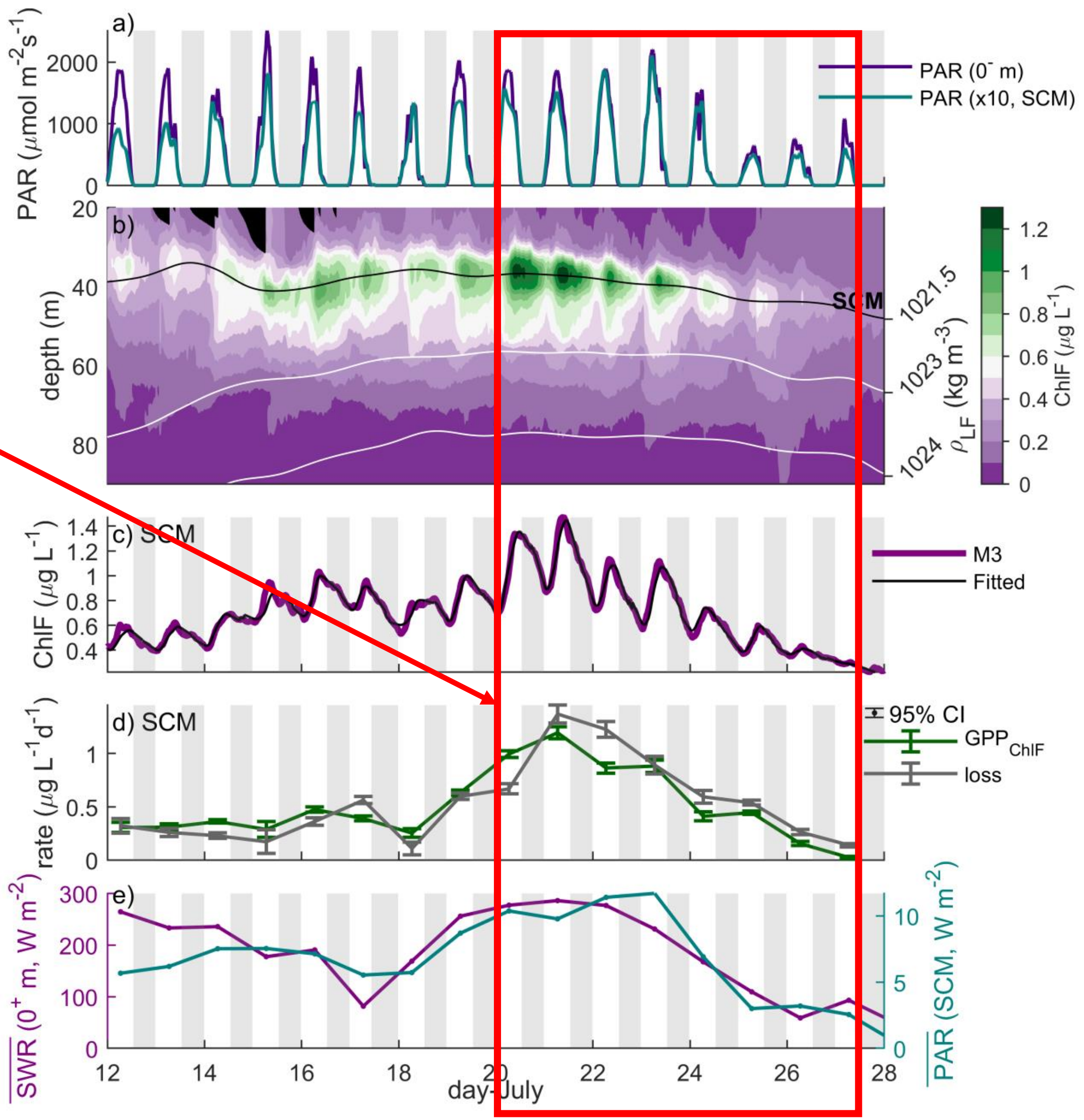

Light-limited production

- SWR vs GPP (top) and PAR vs GPP (bottom) both linearly and significantly ($p<0.001$) related
- PAR better described GPP than SWR, showing time-variable light attenuation (colour) or depth of the SCM is important
- The performance of these fits are surprising given we ignore nutrient limitations

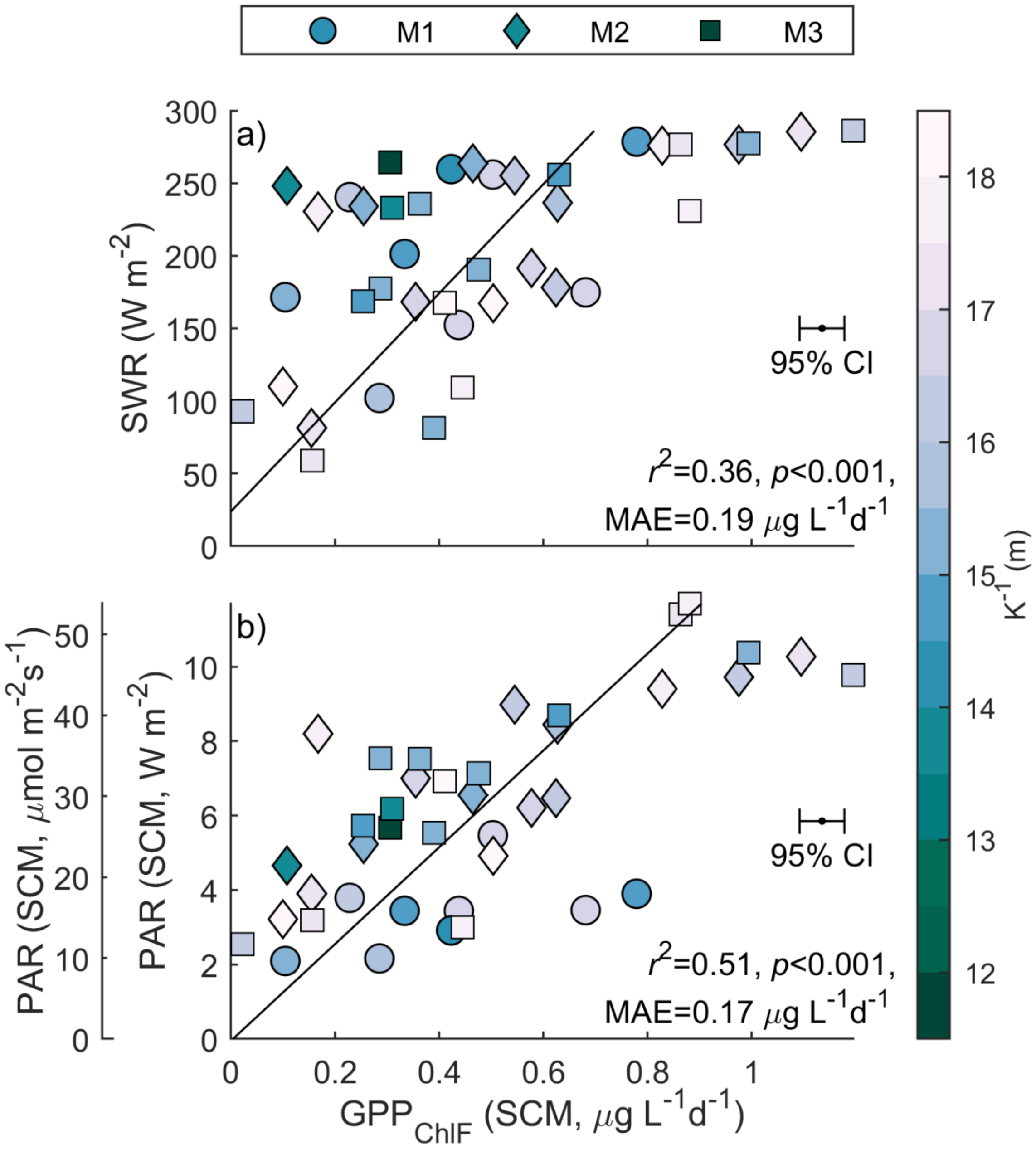

Regional Context

- Southwest monsoon has lower average shortwave radiation but also higher surface Chl
- Typically light-limited??
- Previous studies have shown transition from nutrient- to light-limited growth during the southwest monsoon (Prasanna Kumar et al., 2010)

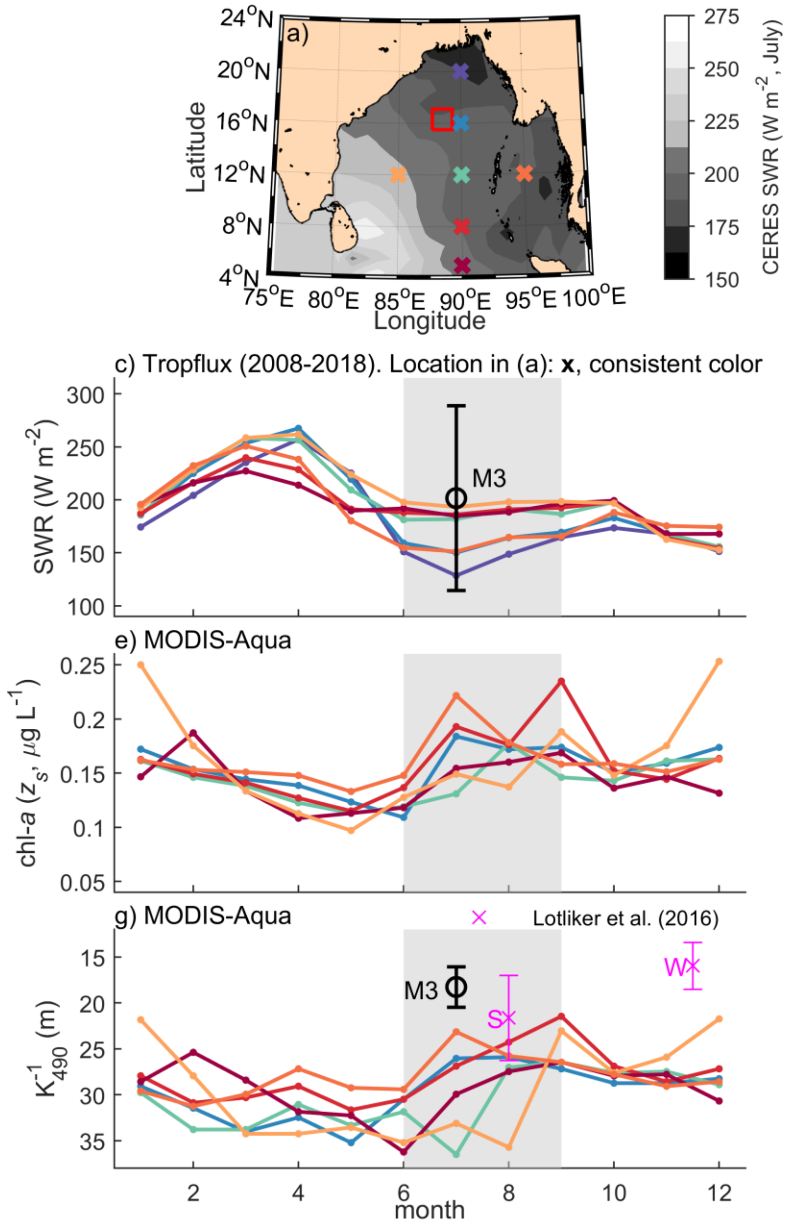

Regional Context

- We additionally consider BGC-Argo observations in the BoB

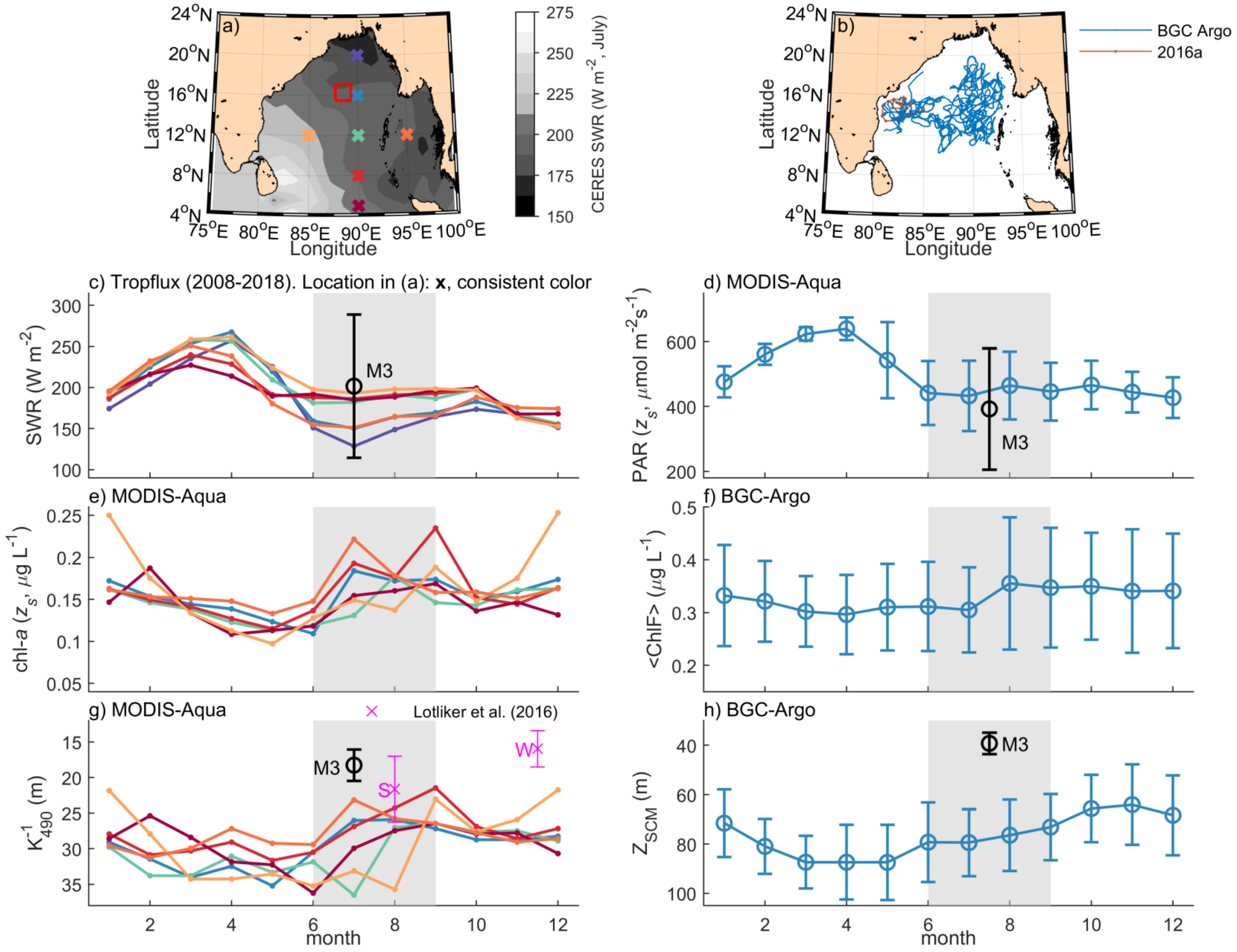

Finding light-limited growth from BGC-Argo

- Surface PAR and ChlF significantly correlated during the southwest monsoon for one profile
- Subsurface irradiance was dependent on cloudiness, a characteristic of the monsoon, and water clarity, which reduced within a coastal plume and a Chl bloom
- Chl concentrations are tightly connected to, and well predicted by, optical observations of subsurface irradiance
- As a result of the monsoon-influenced PAR, there is an intra-seasonal signal in subsurface ChlF

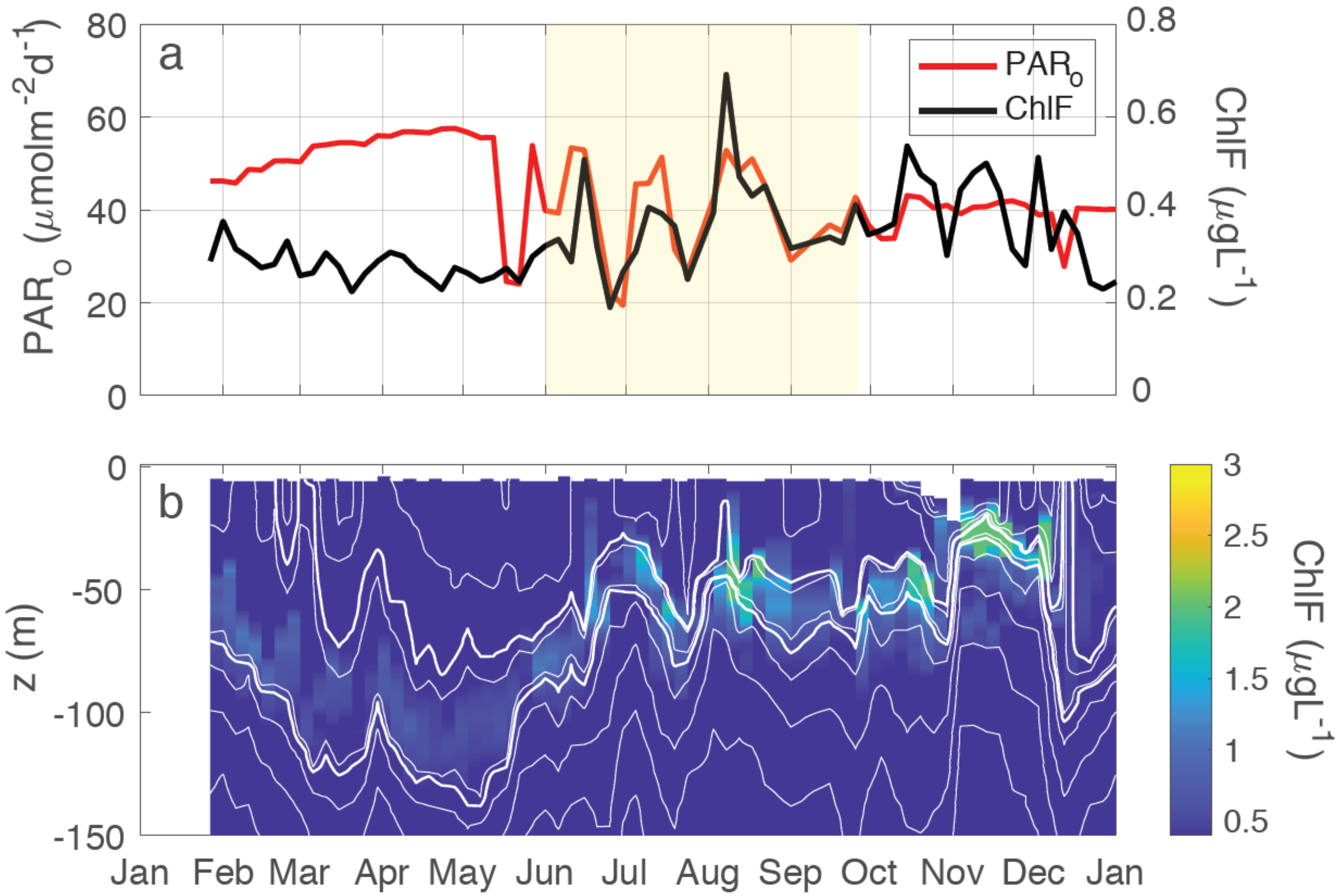

Schlosser et al. (in preparation)

Light-limited phytoplankton growth within the Bay of Bengal during the southwest monsoon (Schlosser et al. in preparation)

Impact of time-variable light attenuation on the upper-ocean heat budget in the Bay of Bengal within one-dimensional coupled air-sea models.
(Future work)

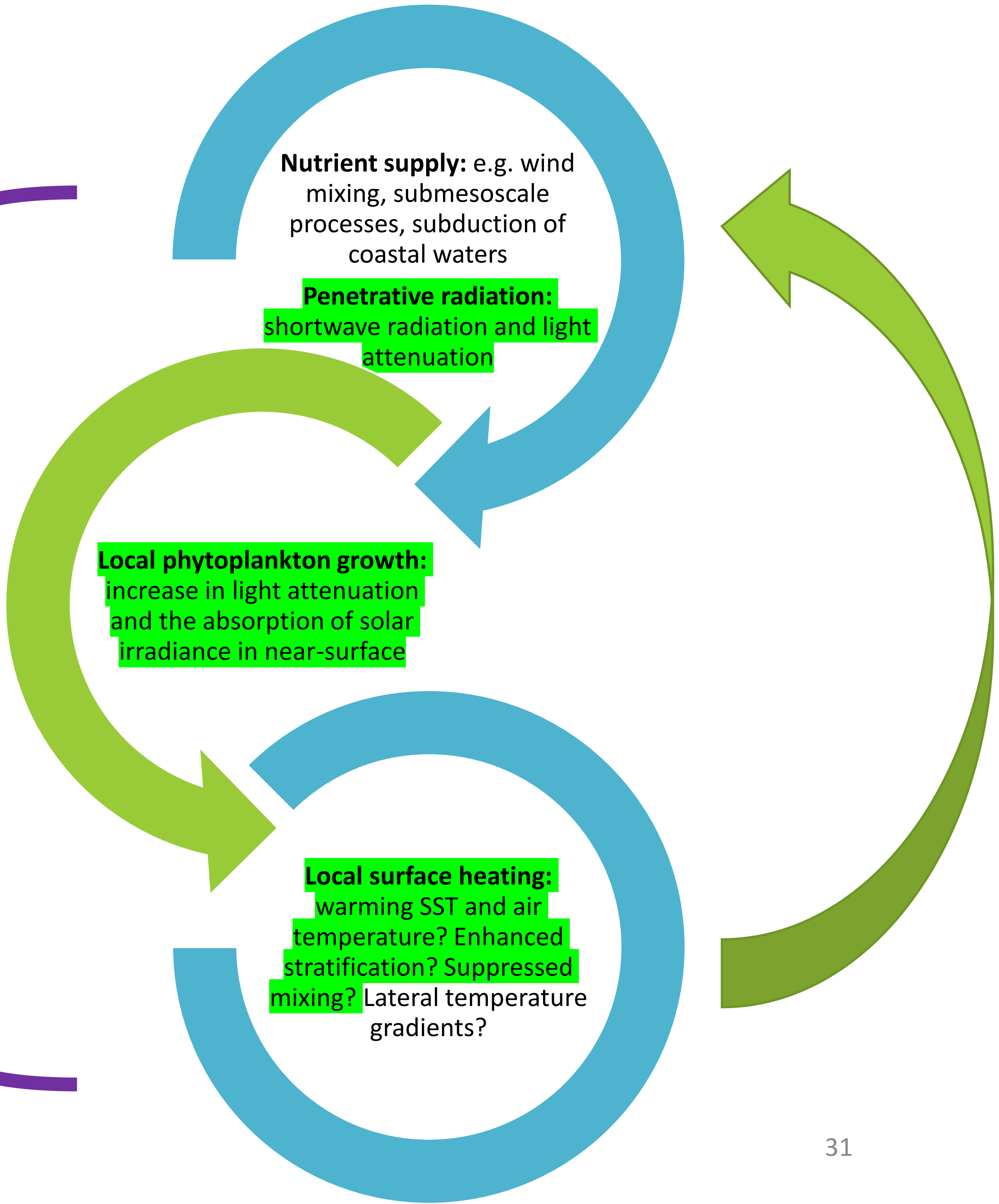

Does $\boldsymbol{K_2(x, y, z, t)}$ impact SST in the BoB?

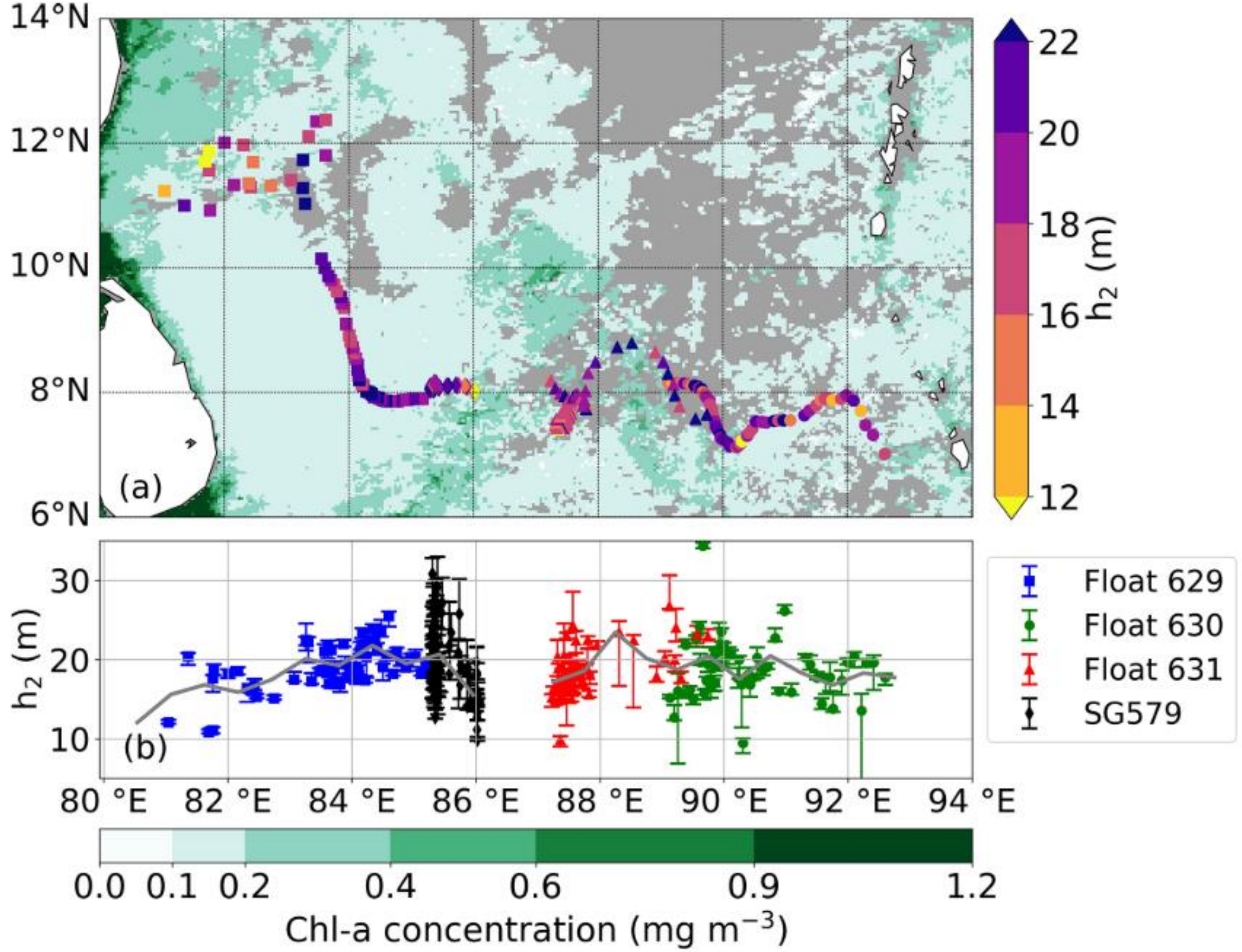

(Giddings et al. 2021)

Sensitivity to K_2 in 1D KPP models

- During the southwest monsoon, Jerlov water type 1B is appropriate (h_2=17 m)
- When ΔMLD is larger, ΔSST also increases

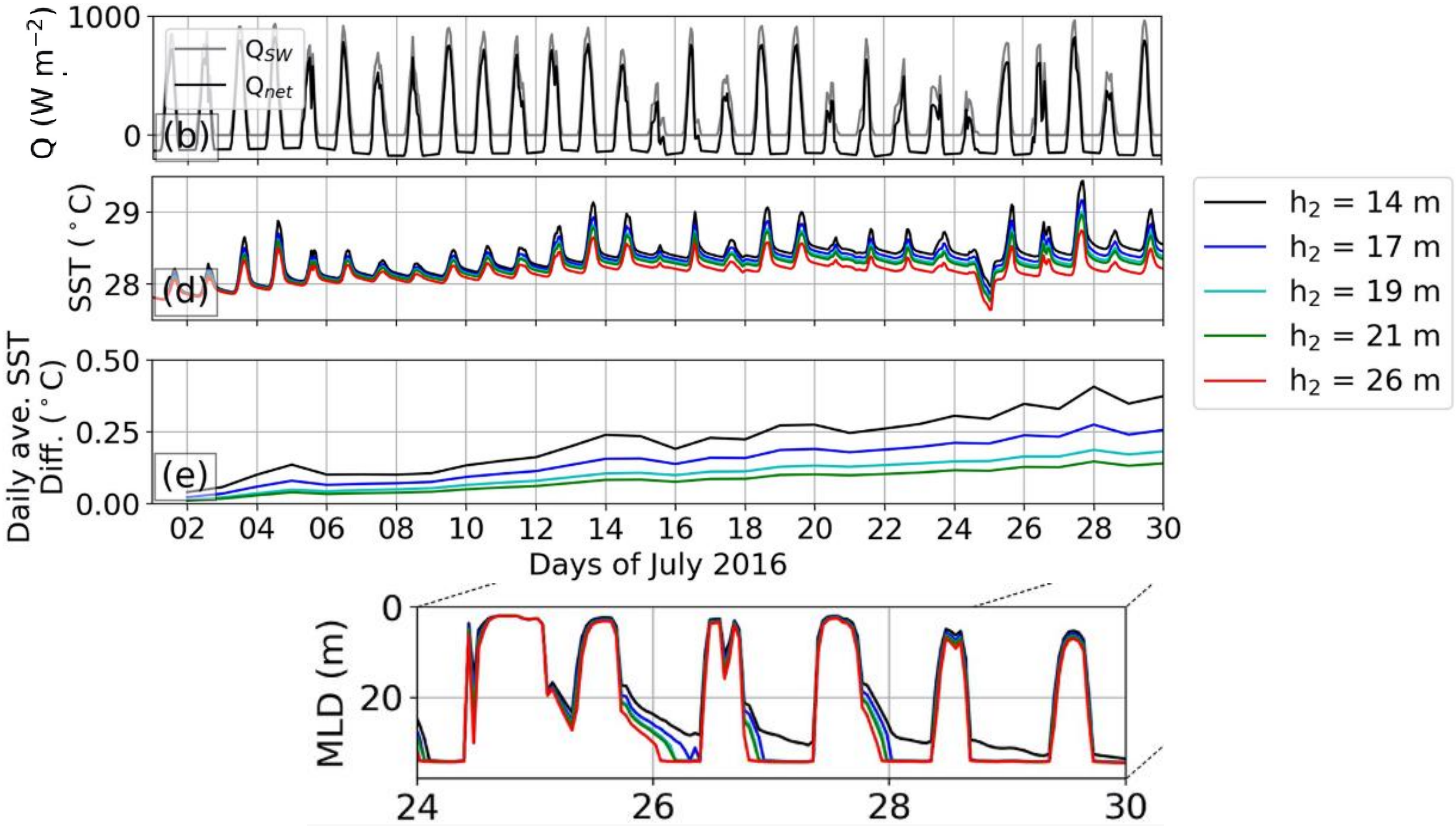

(Giddings et al. 2021)

Significance of ΔSST

- The intra-seasonal SST anomalies during July 1-15 were 0.6°C
- Higher surface Chl (and lower h_2) could generate ~60% of this intra-seasonal variability in SST (Giddings et al. 2021)
- Indicative of potential uncertainty when using a single Jerlov water type for entire BoB

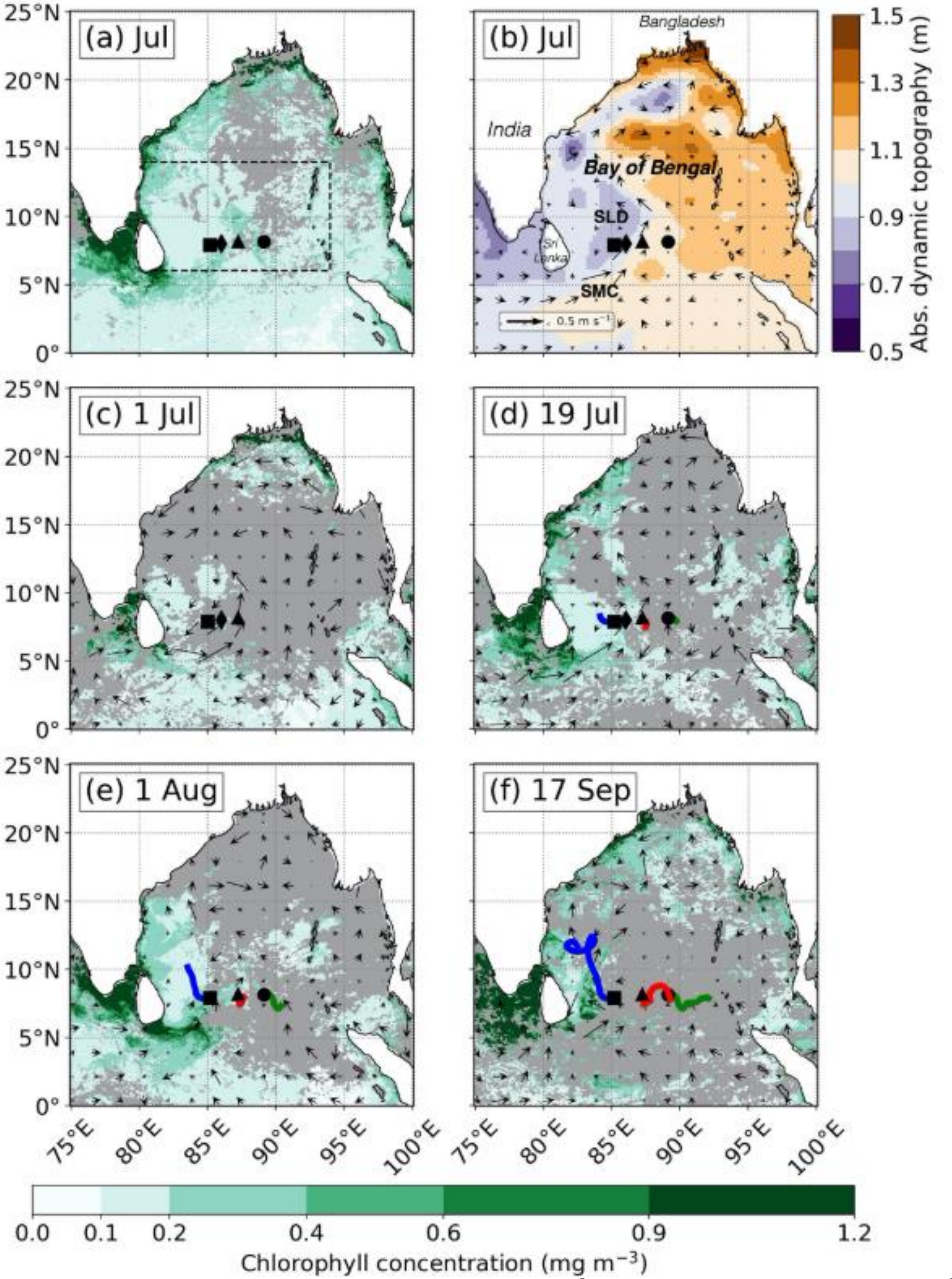

(Giddings et al. 2021)

GOTM idealised 1D modeling

- Collaborating with Leah Johnson

- We test the effect of running GOTM with different light attenuation coefficients and using the KPP-CVmix turbulence scheme:
  - obsK: Observed $\boldsymbol{K_2(t)}$ [10.7 m to 18.1 m], $K_1 = 0.9$, $R = 0.4$ (from Lotliker et al. 2016)
  - meanK: Observed **average** K_2 [15.7 m], $K_1 = 0.9$, $R = 0.4$
  - mink: Observed **minimum** K_2, $K_1 = 0.9$, $R = 0.4$
  - maxK: Observed **maximum** K_2, $K_1 = 0.9$, $R = 0.4$
  - Jerlov water types

Jerlov (1968) water types	R	K_1 (m)	K_2 (m)
Type 1 – relatively clear	0.58	0.35	23
Type 1 (upper 50 m)	0.68	1.2	28
Type 1A	0.62	0.60	20
Type 1B	0.67	1.0	17
Type 2	0.77	1.5	14
Type 3 – murky	0.78	1.4	7.9

Observed range

Preliminary results

- ΔSST progressively increase over break period then rapidly converge after the transition to active conditions

$$\dot{\Theta} = \boxed{\mathcal{D}_\Theta} - \frac{1}{\tau_R^\Theta}(\Theta - \Theta_{obs}) - \boxed{\frac{1}{C_p\rho_0}\frac{\partial I}{\partial z}} \, ,$$

- Changing K_2 within observed range resulted in ΔSST of up to 0.2°C

- Changing R and K_1 resulted in ΔSST of up to 0.6°C (obsK vs jerlov-1b)

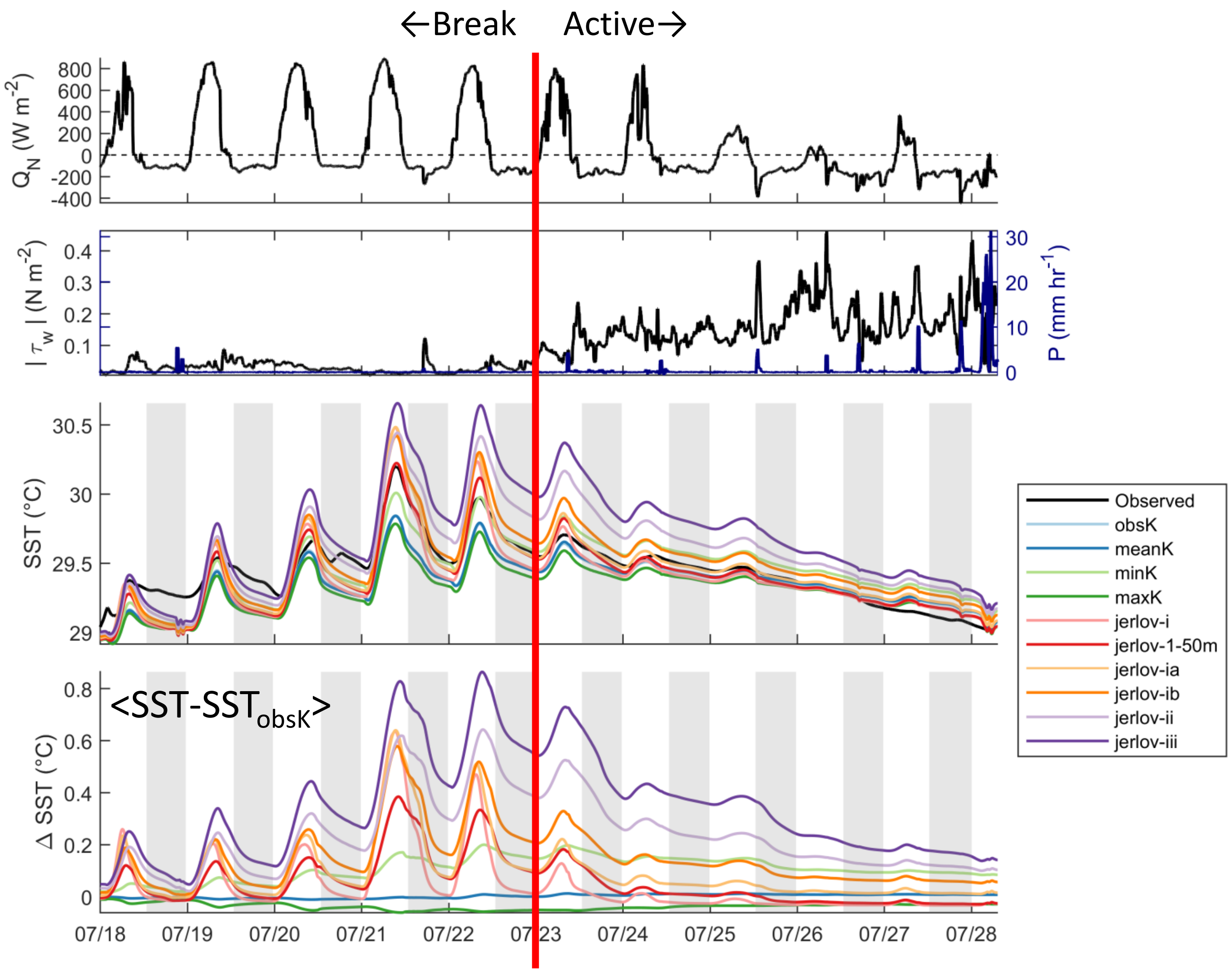

Preliminary results

- ΔMLD of ~15 m at night during break conditions
- ΔMLD progressively decreases over active period
- Diel SST differences increase over break period before sharply converging during active conditions

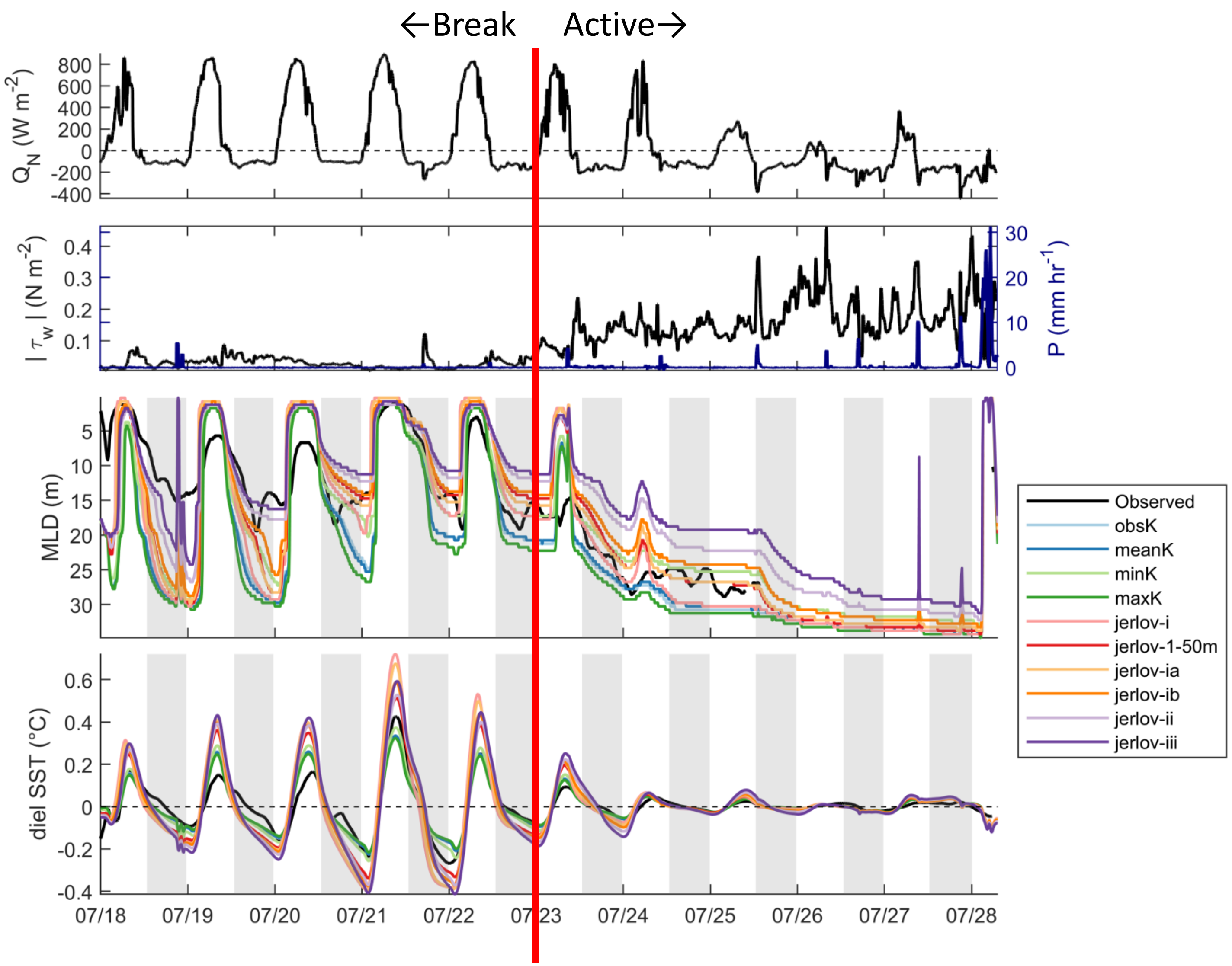

Lateral variability in optics

- We frequently observed variable Chl and/or turbidity around sub-mesoscale features
- In low wind conditions, does K_2 influence lateral gradients in SST?

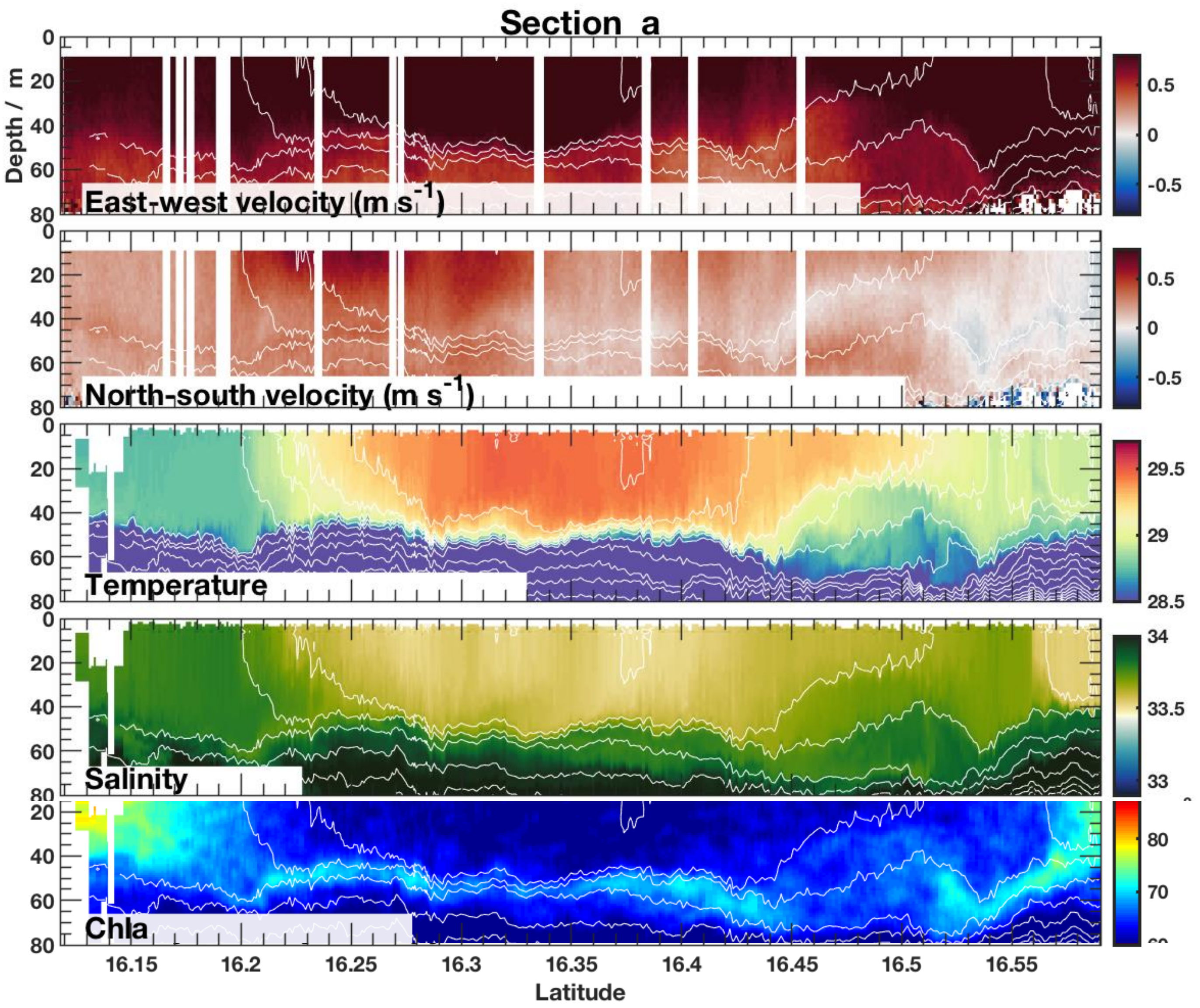

(Produced by Jen MacKinnon)

Conclusions

- The physics and biology are inter-linked, even in the relatively low Chl BoB
- Chl, turbidity, as well as other constituents that impact the water optics, are more likely to influence estimates of SST and MLD during the calm break conditions
- The 3-dimensionality, including the influence of submesoscale processes, needs further investigation

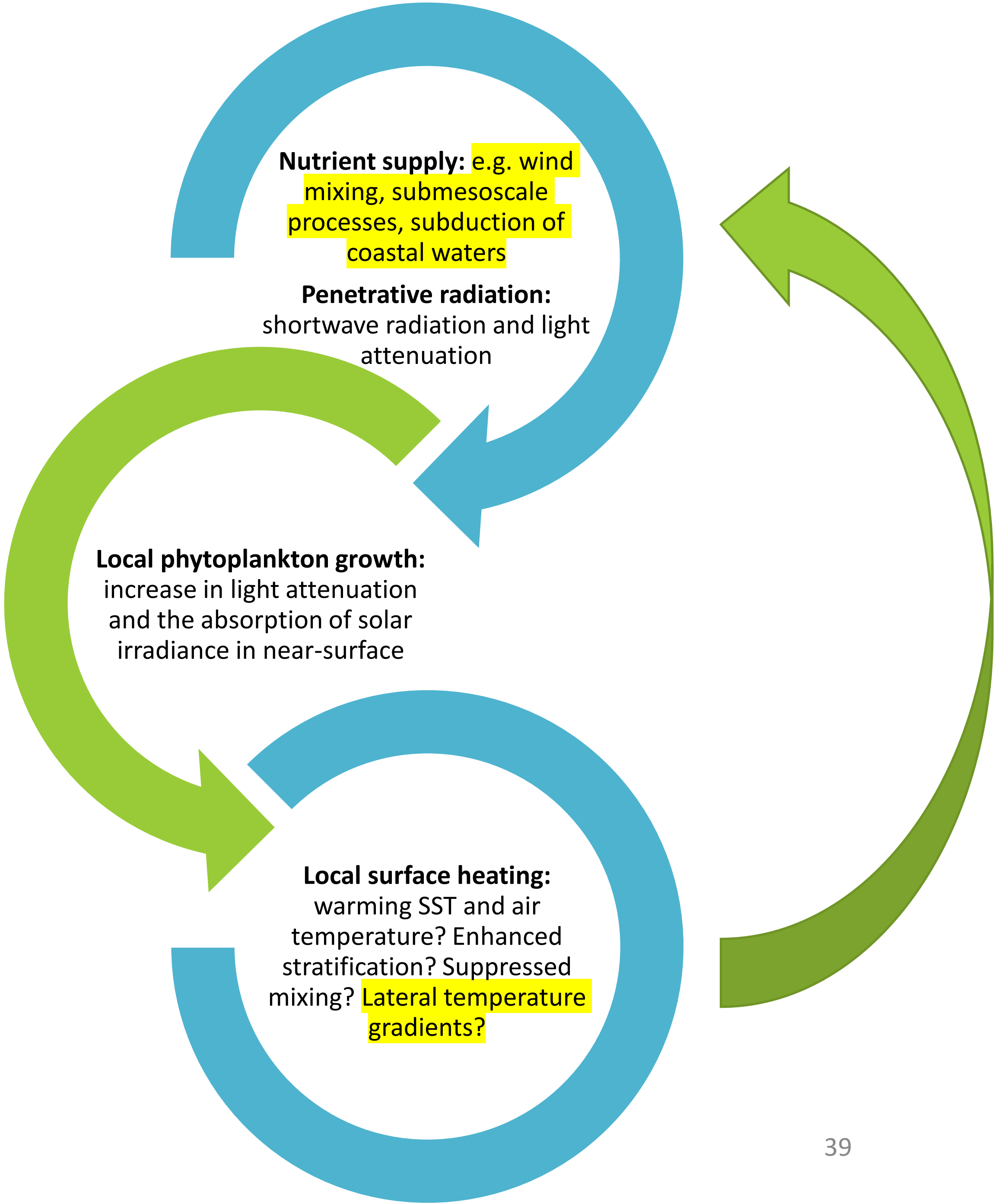

Acknowledgements

Big thank you to crew and science personnel from the R/V Revelle and R/V Sally Ride!